


## RESEARCH ARTICLE

WILEY

The Journal of  
Comparative Neurology

# Differential neuronal and glial expression of nuclear factor I proteins in the cerebral cortex of adult mice

Kok-Siong Chen<sup>1</sup> | Lachlan Harris<sup>2</sup> | Jonathan W. C. Lim<sup>1</sup> | Tracey J. Harvey<sup>2</sup> |  
Michael Piper<sup>1,2</sup> | Richard M. Gronostajski<sup>3</sup> | Linda J. Richards<sup>1,2</sup> | Jens Bunt<sup>1</sup> 

<sup>1</sup>The Queensland Brain Institute, The University of Queensland, Brisbane, Queensland, Australia

<sup>2</sup>The School of Biomedical Sciences, The University of Queensland, Brisbane, Queensland, Australia

<sup>3</sup>Department of Biochemistry, Program in Genetics, Genomics and Bioinformatics, Center of Excellence in Bioinformatics and Life Sciences, State University of New York at Buffalo, Buffalo, New York

## Correspondence

Jens Bunt, The Queensland Brain Institute,  
The University of Queensland, Brisbane,  
Queensland 4072, Australia.

Email: j.bunt@uq.edu.au or  
Linda J. Richards, The Queensland Brain  
Institute, The University of Queensland,  
Brisbane, Queensland 4072, Australia.  
Email: richards@uq.edu.au

## Funding information

Australian Research Council, Grant/Award  
Number: DP140101499, DP106100368,  
FT120100170, and LE100100074; National  
Health and Medical Research Council of  
Australia, Grant/Award Number:  
GNT1100443, GNT1005751, and  
GNT1022308; NYSTEM, Grant/Award  
Number: C026714, C026429, and  
C030133; International Postgraduate  
Student Scholarship from The University of  
Queensland; International Postgraduate  
Research Scholarship from the Australian  
Government; UQ Centennial Scholarship;  
Australian Postgraduate Award from the  
Australian Government; UQ Major  
Equipment and Infrastructure Grant to  
Queensland Brain Institute

## Abstract

The nuclear factor I (NFI) family of transcription factors plays an important role in the development of the cerebral cortex in humans and mice. Disruption of nuclear factor IA (NFIA), nuclear factor IB (NFIB), or nuclear factor IX (NFIX) results in abnormal development of the corpus callosum, lateral ventricles, and hippocampus. However, the expression or function of these genes has not been examined in detail in the adult brain, and the cell type-specific expression of NFIA, NFIB, and NFIX is currently unknown. Here, we demonstrate that the expression of each NFI protein shows a distinct laminar pattern in the adult mouse neocortex and that their cell type-specific expression differs depending on the family member. NFIA expression was more frequently observed in astrocytes and oligodendroglia, whereas NFIB expression was predominantly localized to astrocytes and neurons. NFIX expression was most commonly observed in neurons. The NFI proteins were equally distributed within microglia, and the ependymal cells lining the ventricles of the brain expressed all three proteins. In the hippocampus, the NFI proteins were expressed during all stages of neural stem cell differentiation in the dentate gyrus, with higher expression intensity in neuroblast cells as compared to quiescent stem cells and mature granule neurons. These findings suggest that the NFI proteins may play distinct roles in cell lineage specification or maintenance, and establish the basis for further investigation of their function in the adult brain and their emerging role in disease.

## KEYWORDS

astrocyte, cerebral cortex, cortex, glia, hippocampus, microglia, neuron, NFIA, NFIB, NFIX, nuclear factor I, oligodendrocyte, RRID: AB\_1854421, RRID: AB\_1854424, RRID: AB\_10608433, RRID: AB\_10712361

## 1 | INTRODUCTION

The nuclear factor I (NFI) family of transcription factors plays an important role in brain development (Campbell et al., 2008; das Neves et al., 1999; Driller et al., 2007; Harris, Genovesi, Gronostajski, Wainwright, & Piper, 2015; Jezela-Stanek et al., 2016; Ji, Salamon, & Quintero-Rivera, 2014; Lu et al., 2007; Malan et al., 2010; Nyboe, Kreiborg, Kirchhoff, & Hove, 2015; Piper et al., 2009; Priolo et al., 2012; Sajan

et al., 2013; Shu, Butz, Plachez, Gronostajski, & Richards, 2003; Steele-Perkins et al., 2005). In mouse models, disruption of *Nfia*, *Nfib*, or *Nfix* results in a number of brain phenotypes, including defects of the corpus callosum (das Neves et al., 1999; Driller et al., 2007; Piper et al., 2009; Shu et al., 2003; Steele-Perkins et al., 2005), enlarged ventricles (Campbell et al., 2008; das Neves et al., 1999; Driller et al., 2007; Steele-Perkins et al., 2005), and malformation of the hippocampus (Campbell et al., 2008; Harris et al., 2013; Piper et al., 2009; Shu et al.,

2003; Steele-Perkins et al., 2005). Clinically, similar neurodevelopmental defects are observed in humans when one allele of *NFIA*, *NFIB*, or *NFIX* is mutated or deleted (Jezela-Stanek et al., 2016; Ji et al., 2014; Lu et al., 2007; Malan et al., 2010; Nyboe et al., 2015; Priolo et al., 2012; Sajan et al., 2013). Hence, the function of these proteins as delineated in mouse models appears to be conserved in humans.

During embryonic and early postnatal brain development, *NFIA*, *NFIB*, and *NFIX* proteins are expressed in the dorsal telencephalon (Bunt, Lim, Zhao, Mason, & Richards, 2015; Chaudhry, Lyons, & Gronostajski, 1997; Plachez et al., 2008), with expression reported in radial glia (Betancourt, Katzman, & Chen, 2014; Bunt et al., 2015; Plachez et al., 2008), intermediate progenitors (Betancourt et al., 2014; Campbell et al., 2008; Piper et al., 2010), neurons (Barry et al., 2008; Betancourt et al., 2014; Plachez et al., 2008; Zheng et al., 2010), and glial cells (Plachez et al., 2008; Shu et al., 2003). Their expression is essential for the regulation of cellular proliferation and differentiation in the cortex, hippocampus, cerebellum, and spinal cord (Barry et al., 2008; Betancourt et al., 2014; Deneen et al., 2006; Heng et al., 2014, 2015; Piper et al., 2009, 2010, 2011, 2014). Deletion of *Nfia*, *Nfib*, or *Nfix* in mice causes an increase in the number of radial glia within the neocortex and hippocampus, resulting in reduced and delayed differentiation of neurons and astrocytes (Barry et al., 2008; Betancourt et al., 2014; Heng et al., 2014, 2015; Piper et al., 2009, 2010, 2014). However, as *Nfia*, *Nfib*, and *Nfix* knockout mice usually die before weaning (Campbell et al., 2008; das Neves et al., 1999; Steele-Perkins et al., 2005), the function of the NFI proteins has not been widely studied in the context of the adult brain and their expression has only been investigated in the adult olfactory bulb (Plachez et al., 2012) and subventricular zone (Plachez et al., 2008, 2012).

Considering that NFI proteins have recently been implicated in diseases such as autism and cancer (Chuang, Huang, & Hsueh, 2015; Fancy, Glasgow, Finley, Rowitch, & Deneen, 2012; Genovesi et al., 2013; Glasgow et al., 2013; Ho et al., 2013; Idbaih et al., 2008; Lacroix et al., 2014; Lastowska et al., 2013; Le-Niculescu et al., 2009; Lee et al., 2014; Song et al., 2010; Stringer et al., 2016; Suwarnalata et al., 2016; Tsang et al., 2013; Vyazunova et al., 2014), a thorough analysis of their expression in the adult brain is required. Here, we examined both region and cell-type-specific expression in the adult mouse cerebral cortex using antibodies specific for *NFIA*, *NFIB*, and *NFIX*. This analysis provides a basis for further study of NFI function in healthy and diseased brains.

## 2 | MATERIALS AND METHODS

### 2.1 | Animals and brain tissue collection

All mice were housed and handled in accordance with the Australian Code of Practice for the Care and Use of Animals for Scientific Purposes and with approval from the institutional Animal Ethics Committee. C57BL/6J (RRID:IMSR\_JAX:000664), *Nfiatm1Rmg* (das Neves et al., 1999) (*Nfia*<sup>-/-</sup>; RRID:MGI:2449024), *Nfib*<sup>tm1Rmg</sup> (Steele-Perkins et al., 2005) (*Nfib*<sup>-/-</sup>; RRID:MGI:3530497), *Nfix*<sup>tm1.1Rmg</sup> (Campbell et al., 2008) (*Nfix*<sup>-/-</sup>; RRID:MGI:3802571), and *ICR.Cg-Gad1*<sup>tm1.1Tama</sup> (Tamamaki et al., 2003) (GAD67-GFP; RRID:IMSR\_RBRC03674) mice were housed

on a 12 hr dark/light cycle with water and food provided ad libitum. Animals were transcardially perfused with saline, followed by 4% w/v paraformaldehyde solution, as previously described (Piper et al., 2011).

### 2.2 | Antibody characterization

All antibodies used in this study are listed in Table 1.

#### 2.2.1 | Nuclear factor 1A

The rabbit polyclonal anti-nuclear factor 1A (NFIA) antibody (Sigma-Aldrich, St Louis, MO; Cat# HPA008884, RRID:AB\_1854421) specifically detects a single band at ~58 kDa on Western blots of U251 glioma cell lysates (manufacturer's information). To test the specificity of this antibody for immunohistochemistry (IHC), *Nfia*<sup>-/-</sup> and wild-type brain sections were stained. No specific nuclear staining was detected in the knockout brains (Figure 1a,b).

#### 2.2.2 | Nuclear factor 1B

The rabbit polyclonal anti-nuclear factor 1B (NFIB) antibody (Sigma-Aldrich; Cat# HPA003956, RRID:AB\_1854424) detects NFIB protein expression by IHC of U-251 MG cells (manufacturer's information). The specificity of the antibody was tested with IHC on *Nfib*<sup>-/-</sup> and wild-type brain sections. No specific nuclear staining was detected in the knockout brains (Figure 1c,d).

#### 2.2.3 | Nuclear factor 1X

The specificity of the mouse monoclonal anti-nuclear factor 1X (NFIX) antibody (Sigma-Aldrich; Cat# SAB1401263, RRID:AB\_10608433) was tested with IHC on *Nfix*<sup>-/-</sup> and wild-type brain sections. No specific nuclear staining was seen in the knockout tissue (Figure 1e,f). The rabbit polyclonal anti-NFIX antibody (Abcam, Cambridge, UK; Cat# ab101341, RRID:AB\_10712361) was previously characterized with IHC on *Nfix*<sup>-/-</sup> and wild-type brain sections. No specific nuclear staining was detected in the knockout brains (Harris et al., 2013).

#### 2.2.4 | NeuN

The mouse monoclonal NeuN antibody A60 (Millipore, Bedford, MA; Cat# MAB377, RRID:AB\_2298772) specifically recognizes the protein NeuN, a neuronal marker that is expressed in most neuronal cell types. Immunoreactivity is detected as specific nuclear staining in neurons in the cerebral cortex (Mullen, Buck, & Smith, 1992). This antibody has been extensively used to label neuronal cell types, with 119 citations listed at the time of manuscript preparation in the Journal of Comparative Neurology Antibody Database (RRID:SCR\_006470).

#### 2.2.5 | Green fluorescent protein

The chicken polyclonal anti-green fluorescent protein (GFP) antibody (Abcam; Cat# ab13970, RRID:AB\_300798) was used to label GFP expressed in interneurons in adult GAD67-GFP mice. This antibody recognized a single band of ~30 kDa on Western blots of extracts from GFP-expressing mouse kidney cells (Grimm, Foutz, Brenner, & Sansom, 2007) and specifically stained GFP-expressing cells using immunofluorescence on murine olfactory epithelium tissue, spinal cord olfactory bulb, and mouse brain tissues (manufacturer's information).

**TABLE 1** Primary antibody dilutions used for immunohistochemistry (IHC) or immunofluorescence (IF) in this study

Antibody	Description of immunogen	Host	Dilution	Source.RRID
Nuclear factor IA (NFIA)	Recombinant protein corresponding to amino acids 151-261 of human NFIA (NP_005586.1)	Rabbit polyclonal	1/500 (IF)	Sigma-Aldrich, St Louis, MO; Cat# HPA008884, RRID:AB_1854421
			1/750 (IHC)	
Nuclear factor IB (NFIB)	Recombinant protein corresponding to amino acids 239-386 of human NFIB (NP_001177667.1)	Rabbit polyclonal	1/500 (IF)	Sigma-Aldrich, St Louis, MO; Cat# HPA003956, RRID:AB_1854424
			1/750 (IHC)	
Nuclear factor IX (NFIX)	Recombinant protein corresponding to amino acids 291-391 of human NFIX (NP_002492.2)	Mouse monoclonal	1/2,000 (IF)	Sigma-Aldrich, St Louis, MO; Cat# SAB1401263, RRID:AB_10608433
			1/2,000 (IHC)	
Nuclear factor IX (NFIX)	Recombinant protein corresponding to amino acids 165-330 of human NFIX (NP_002492.2)	Rabbit polyclonal	1/100 (IF)	Abeam, Cambridge, UK; Cat#abl01341, RRID:AB_10712361
NeuN	Purified cell nuclei from mouse brain, clone A60	Mouse monoclonal	1/700 (IF)	Millipore, Bedford, MA; Cat# MAB377, RRID:AB_2298772
Green fluorescent protein (GFP)	Recombinant full length protein corresponding to GFP	Chicken polyclonal	1/500 (IF)	Abeam, Cambridge, UK; Cat# abl3970, RRID:AB_300798
Glial fibrillary acidic protein (GFAP)	Purified full length native protein corresponding to cow GFAP	Chicken polyclonal	1/1,000 (IHC)	Abeam, Cambridge, UK; Cat# ab4674, RRID:AB_304558
S100 calcium-binding protein B (S100B)	Purified bovine brain S100 protein, clone 4C4.9	Mouse monoclonal	1/500 (IF)	Abeam, Cambridge, UK; Cat# ab4066, RRID:AB_304258
Oligodendrocyte lineage transcription factor 2 (OLIG2)	Purified peptide corresponding to amino acids 300-350 of mouse OLIG2 (Q9EQW6)	Goat polyclonal	1/200 (IF)	Santa Cruz, Dallas, TX; Cat# sc-19969, RRID:AB_2236477
Ionized calcium-binding adapter molecule 1 (IBA1)	Synthetic peptide corresponding to amino acids 135-147 of human IBA1 (NP_001614.3)	Goat polyclonal	1/1,000 (IF)	Abeam, Cambridge, UK; Cat# ab5076, RRID:AB_2224402
Forkhead box J1 (FOXJ1)	Purified protein from mouse, clone 2A5	Mouse monoclonal	1/1,000 (IF)	eBioscience, San Diego, CA; Cat# 149965-82, RRID:AB_1548835
Sex determining region Y-box 2 (SOX2) Alexa Fluor 488 conjugated	Purified protein corresponding to C-terminal region of SOX2, conserved between human and mouse, clone btjce	Rat monoclonal	1/400 (IF)	eBioscience, San Diego, CA; Cat# 539811-82, RRID:AB_2574479
Ki67	Purified protein from human Ki67, clone B56	Mouse monoclonal	1/200 (IF)	BD Biosciences, Sparks, MD; Cat# 550609, RRID:AB_393778
Doublecortin (DCX)	Purified peptide corresponding to amino acids 390-440 of human DCX (043602)	Goat polyclonal	1/200 (IF)	Santa Cruz, Dallas, TX; Cat# sc-8066, RRID:AB_2088494

## 2.2.6 | Glial fibrillary acidic protein

The chicken polyclonal anti-glial fibrillary acidic protein (GFAP) antibody (Abcam; Cat# ab4674, RRID:AB\_304558) recognizes the intermediate filament GFAP that is expressed in astrocytes in the central nervous system (Eng & Ghimikar, 1994). This antibody detects a band at ~50 kDa on Western blots of mouse brain extract (manufacturer's information). It has previously been used to specifically detect cells of the astrocytic lineage in the developing mouse neocortex and ventral forebrain (Nagao, Ogata, Sawada, & Gotoh, 2016). This antibody also

specifically stains for cells that demonstrate a stellate morphology, characteristic of astrocytes, in neuron-glia cocultures prepared from the developing rat brain (Muller, Stellmacher, Freitag, Landgraf, & Dietrich, 2015).

## 2.2.7 | S100 calcium-binding protein B (S100B)

The mouse monoclonal anti-S100B antibody 4C4.9 (Abcam; Cat# ab4066, RRID:AB\_304258) recognizes S100B, a protein that in the central nervous system is predominantly expressed in astrocytes and

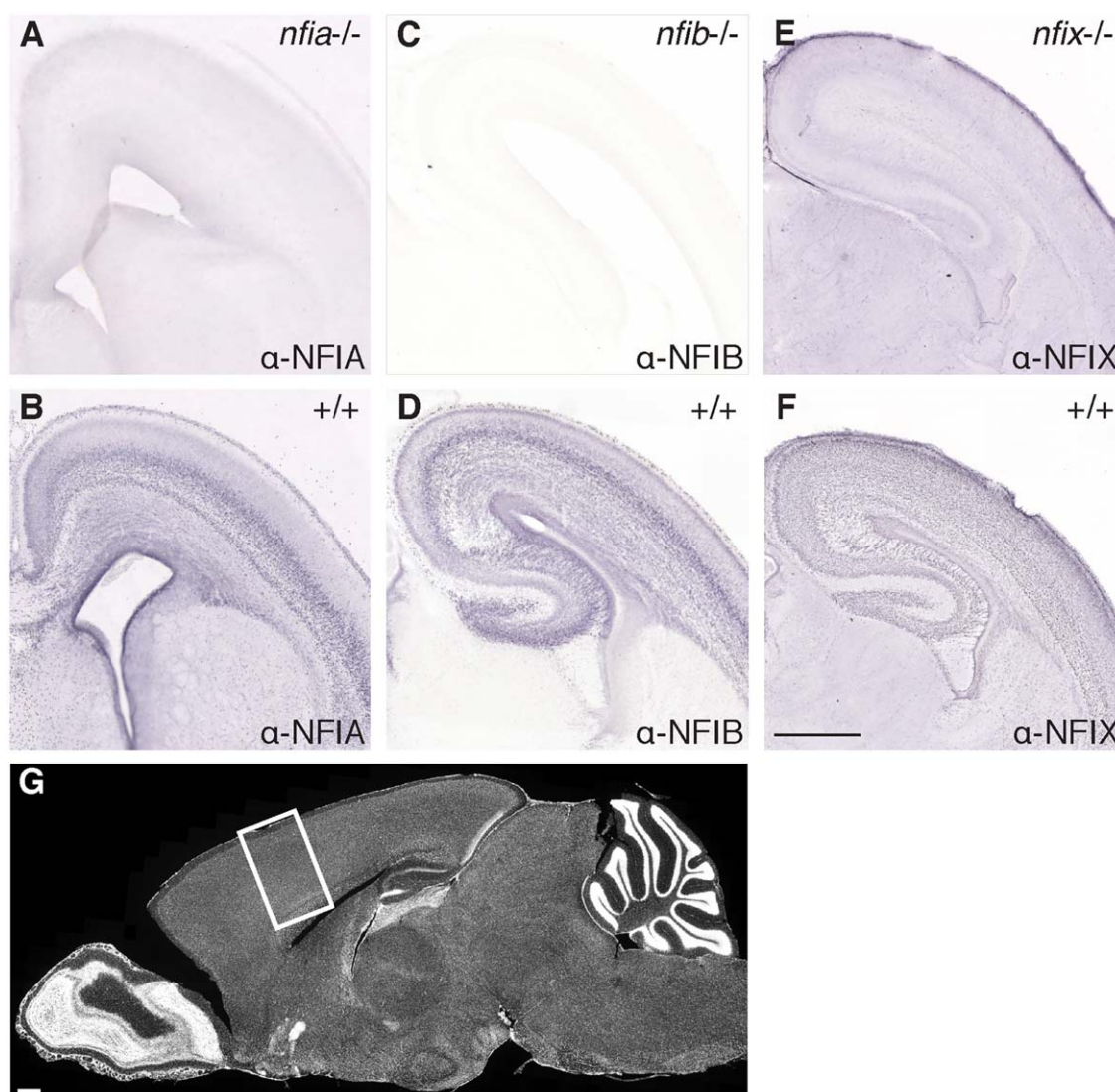


**FIGURE 1** Verification of NFI antibody specificity by immunohistochemistry on knockout brain tissue and schematic representation of the region selected for cell counts. The specificity of the rabbit polyclonal anti-NFIA (RRID:AB\_1854421), rabbit polyclonal anti-NFIB (RRID:AB\_1854424), and mouse monoclonal anti-NFIX (RRID:AB\_10608433) antibodies was determined with nickel-DAB immunostaining on 50  $\mu$ m coronal vibratome sections of *Nfia* (a), *Nfib* (c), or *Nfix* (e) E18 knockout mice, respectively, and their corresponding wild-type littermates (b, d, f, respectively). No specific labeling could be detected in any knockout tissue. (g) The boxed region represents the region of interest (ROI) that was identically placed on all midline sagittal sections for cell counting throughout this study. Scale bar = 500  $\mu$ m in (f) for (a–f); 500  $\mu$ m in (g). [Color figure can be viewed at [wileyonlinelibrary.com](http://wileyonlinelibrary.com)]

was used as an astrocytic marker in this study. The specificity of this antibody was previously determined with immunofluorescence in S100B knockout and wild-type brain tissue, with no staining reported in the knockout tissue (Tanga, Raghavendra, Nutile-McMenemy, Marks, & Deleo, 2006).

## 2.2.8 | Oligodendrocyte lineage transcription factor 2

The goat polyclonal anti-oligodendrocyte lineage transcription factor 2 (OLIG2) antibody (Santa Cruz, Dallas, TX; Cat# sc-19969, RRID:AB\_2236477) recognizes the transcription factor OLIG2 that is expressed in cells of the oligodendrocytic lineage (Clase et al., 2006; Desfeux et al., 2010). This antibody recognizes a band at ~40 kDa on Western blots of mouse brain tissue extract (manufacturer's informa-

tion). This antibody was also used previously to differentiate between oligodendroglia and microglia in the grey matter of the brain stem and the white matter of the corpus callosum in the adult mouse brain (Clase et al., 2006).

## 2.2.9 | Ionized calcium-binding adapter molecule 1

The goat polyclonal anti-ionized calcium-binding adapter molecule 1 (IBA1) antibody (Abcam; Cat# ab5076, RRID:AB\_2224402) recognizes IBA1, a protein that is expressed in microglia (Ito et al., 1998) and was used as a marker of this cell type. This antibody recognized a band at ~17 kDa on Western blots of mouse spleen tissue lysate (manufacturer's information). It was previously demonstrated to specifically label activated microglia in irradiated mouse brains (Kalm, Lannering, Bjork-



Eriksson, & Blomgren, 2009) and we validated the staining specificity using a microglial reporter mouse model (Parkhurst et al., 2013).

### 2.2.10 | Forkhead box J1

The mouse monoclonal anti-forkhead box J1 (FOXJ1) antibody 2A5 (eBioscience, San Diego, CA; Cat# 14-9965-82, RRID:AB\_1548835) recognizes the transcription factor FOXJ1 that is required for the differentiation of ependymal cells (Jacquet et al., 2009) and was used as an ependymal marker in this study. This antibody detected a single ~58 kDa band on Western blots of mouse tracheal epithelial lysates (manufacturer's information). The nuclear localization of FOXJ1 immunoreactivity in ependymal cells observed in this study (Figure 8i-l) was identical to the characterization of ependymal cells in primary cultures of rat cerebral cortex reported previously (Jordan, Rieke, Hughes, & Thomas, 1990).

### 2.2.11 | Sex determining region Y-box 2

The rat monoclonal anti-sex determining region Y-box 2 (SOX2) antibody Btjce (eBioscience; Cat# 53-9811-82, RRID:AB\_2574479) was used as an adult neural progenitor marker. High expression of SOX2 has been reported in adult neural stem cells (Ferri et al., 2004). The nuclear localization of SOX2 immunoreactivity in adult neural stem cells observed in this study (Figure 12a-c) was identical to SOX2 expression as reported previously in the adult mouse brain (Ferri et al., 2004).

### 2.2.12 | Ki67

The mouse monoclonal anti-Ki67 antibody B56 (BD Biosciences, Sparks, MD; Cat#550609, RRID:AB\_393778) was used together with SOX2 to label proliferating neural stem cells. This antibody detects a double band (345 and 395 kDa) in Western blots of proliferating cells (manufacturer's information). The nuclear localization of Ki67 immunoreactivity observed in these cells (Figure 12a-c) was identical to that observed in proliferating cells in the rat dorsal vagal complex (Pecchi et al., 2007).

### 2.2.13 | Doublecortin

The goat polyclonal anti-doublecortin (DCX) antibody (Santa Cruz; Cat# sc-8066, RRID:AB\_2088494) was used as a neuroblast marker. It recognized a single ~43 kDa band in Western blots of mouse embryo extracts and in human neuroblastoma SK-N-SH cells (manufacturer's information). This antibody has been extensively used to label neuroblasts, with 26 citations listed in the Journal of Comparative Neurology Antibody Database (RRID:SCR\_006470). The immunoreactivity of this antibody is similar to three other DCX antibodies in the mouse cerebral cortex (Bloch et al., 2011).

## 2.3 | Tissue processing

### 2.3.1 | Microtome sectioning

Fixed brains of six 9-month old C57BL/6J female mice were paraffin-infiltrated by dehydrating the brains through a series of ethanol (70–100% v/v) and xylene (VWR, Tingalpa, Australia) washes, followed by

three successive paraffin wax changes at 60°C. Following infiltration, the brains were embedded, blocked, and sectioned at 5 µm on a microtome (Leica, Wetzlar, Germany), then mounted on SuperfrostPlus slides. The paraffin sections were deparaffinized and rehydrated by a sequential series of xylene, ethanol, and distilled water washes prior to IHC.

### 2.3.2 | Vibratome sectioning

Following perfusion and post-fixation, the brains of 9-month-old heterozygous *Nfib*<sup>tm1Rmg</sup> mice were embedded in 3–4% w/v Difco Noble agar (Becton, Dickinson and Company, Sparks, MD) in distilled water, and sectioned sagittally at 40 µm on a vibratome (Leica). The sections were then mounted onto SuperfrostPlus slides (Menzel-Gläser, Brunswick, Germany), and dried at room temperature until fully adherent. Sections were post-fixed with 4% w/v paraformaldehyde for 10 min and rehydrated with phosphate buffered saline (PBS) for 5 min prior to IHC.

## 2.4 | Immunohistochemistry

### 2.4.1 | Chromogenic IHC

Chromogenic IHC was conducted as previously described (Plachez et al., 2008) with minor modifications. Brain sections were antigen-retrieved in an antigen decloaking chamber (Biocare Medical, Concord, CA). The sections were heated to 125°C for 4 min at 15 psi in sodium citrate buffer (10 mM C<sub>6</sub>H<sub>5</sub>Na<sub>3</sub>O<sub>7</sub> · 2H<sub>2</sub>O, 0.05% v/v Tween 20 (Sigma-Aldrich) in MilliQ water, pH 6.0). Following antigen retrieval, slides were washed in PBS for 5 min and incubated for 2 hr in blocking solution containing 2% v/v normal donkey serum (Jackson ImmunoResearch Labs, West Grove, PA; Cat# 017-000-001, RRID:AB\_2337254), 0.9% v/v H<sub>2</sub>O<sub>2</sub> (Chem-Supply, Adelaide, Australia), and 0.2% v/v Triton X-100 (Sigma-Aldrich) in PBS. Sections were then incubated overnight with the primary antibody diluted in blocking solution. The primary antibodies are listed in Table 1. The sections were washed in PBS for 3x20 min before incubating with secondary antibody for 1 hr. The secondary antibodies were either biotinylated donkey anti-mouse IgG (Jackson ImmunoResearch Labs; Cat# 715-065-151, RRID:AB\_2340785), biotinylated donkey anti-chicken IgY (Millipore; Cat# AP194B, RRID:AB\_92675), or biotinylated donkey anti-rabbit IgG (Jackson ImmunoResearch Labs; Cat# 711-065-152, RRID:AB\_2340593), diluted in 0.2% v/v Triton X-100 in PBS. The sections were washed for 3x20 min and then incubated for 1 hr in an avidin-biotin complex solution (0.2% v/v Triton X-100, avidin [1 : 500] and biotin [1 : 500] from a Vectastain Elite ABC kit (Vector Laboratories, Burlingame, CA; Cat# PK-6100 RRID:AB\_2336819) in PBS). After 3x10 min washes in PBS, sections were incubated with nickel-3,3'-diaminobenzidine tetrahydrochloride (DAB) chromogen solution (95 mM NiSO<sub>4</sub>, 175 mM C<sub>2</sub>H<sub>3</sub>NaO<sub>2</sub>, 0.56 mM DAB (Sigma-Aldrich), 0.00075% v/v H<sub>2</sub>O<sub>2</sub>). Once visible staining developed, sections were washed in PBS to stop the color reaction. After 3x10 min washes, the sections were dehydrated through a series of ethanol washes (70–100%) and cleared with xylene, for at least 1 min each. Slides were coverslipped with DPX neutral mounting medium (Ajax Finechem, Sydney, Australia).

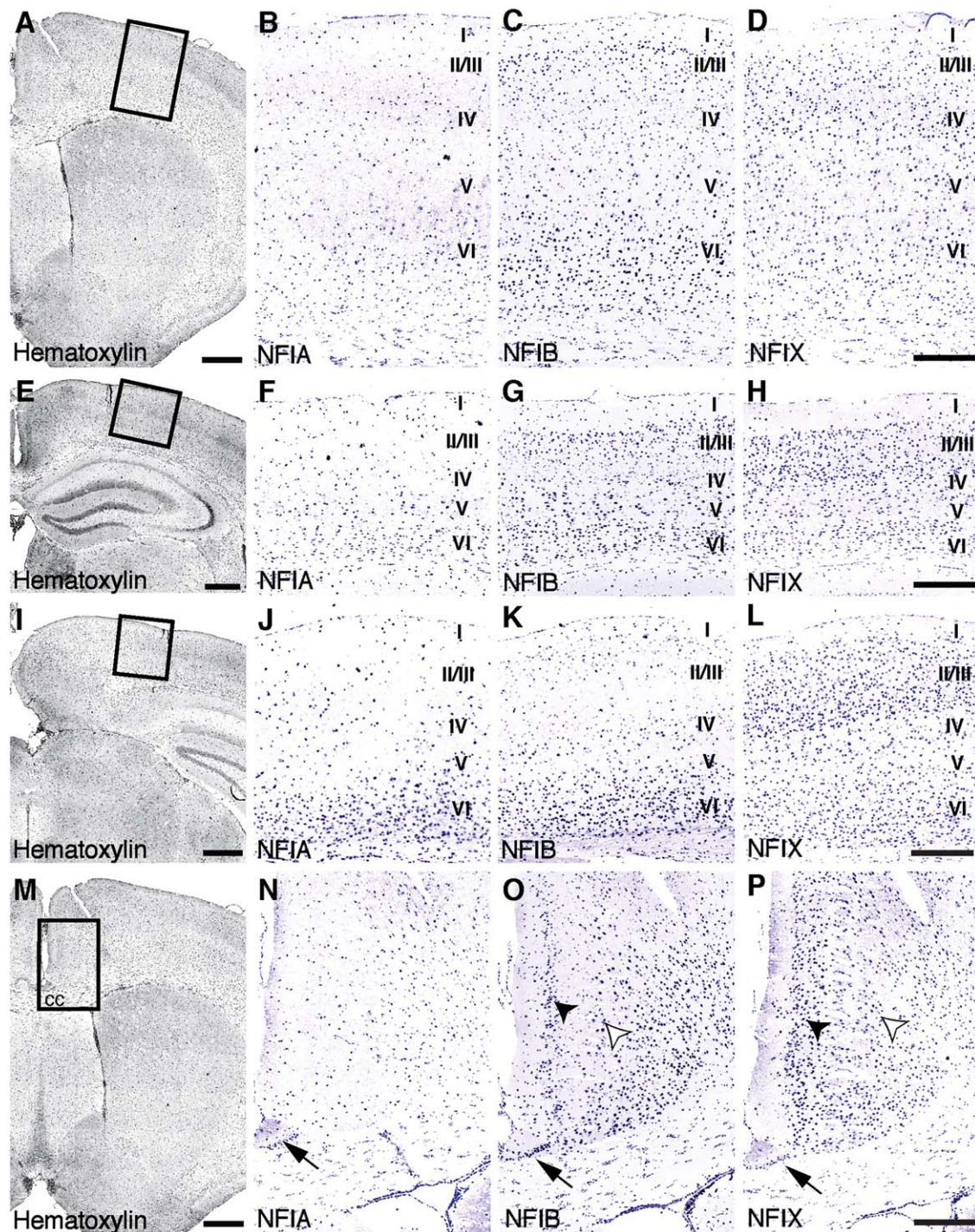


**FIGURE 2** NFI protein expression shows a distinct laminar distribution in the adult neocortex. The expression of NFIA, NFIB, and NFIX proteins was examined with nickel-DAB immunostaining on 5  $\mu$ m paraffin-embedded coronal sections. These sections correspond to rostral in (a–d) (interaural 4.7 mm, Bregma 0.9 mm), middle in (e–h) (interaural 1.9 mm, Bregma –1.9 mm), and caudal in (i–l) (interaural 0.5 mm, Bregma –3.3 mm) obtained from the mouse atlas of Franklin and Paxinos 1997 ( $n = 6$ ). (a–l) The three proteins were expressed throughout the neocortex, with denser cell-labeling observed caudally. Higher NFIA expression was detected in the deeper cortical layers compared to the upper layers (b, f, j). NFIB expression was more localized to layers II/III, V, and VI (c, g, k), whereas NFIX expression was highest in the lower region of layer II/III (d, h, l). (m–p) NFIA expression was sparse in the cingulate cortex (n), whereas NFIB and NFIX were expressed at higher levels just below the marginal zone (closed arrowhead) and in the deeper layers (open arrowhead) (o, p). All three NFI proteins were detected in the corpus callosum and the indusium griseum (arrow) in similar patterns (n–p). The boxed regions represent regions of high magnification: (b–d) for (a); (f–h) for (e); (j–l) for (i); (n–p) for (m). The Roman numerals I, II/III, IV, V, and VI denote the respective cortical layers. CC = corpus callosum. Scale bars = 500  $\mu$ m in (m) for (a), (e), (i), and (m); 250  $\mu$ m in (d), (h), (l), and (p). [Color figure can be viewed at [wileyonlinelibrary.com](http://wileyonlinelibrary.com)]



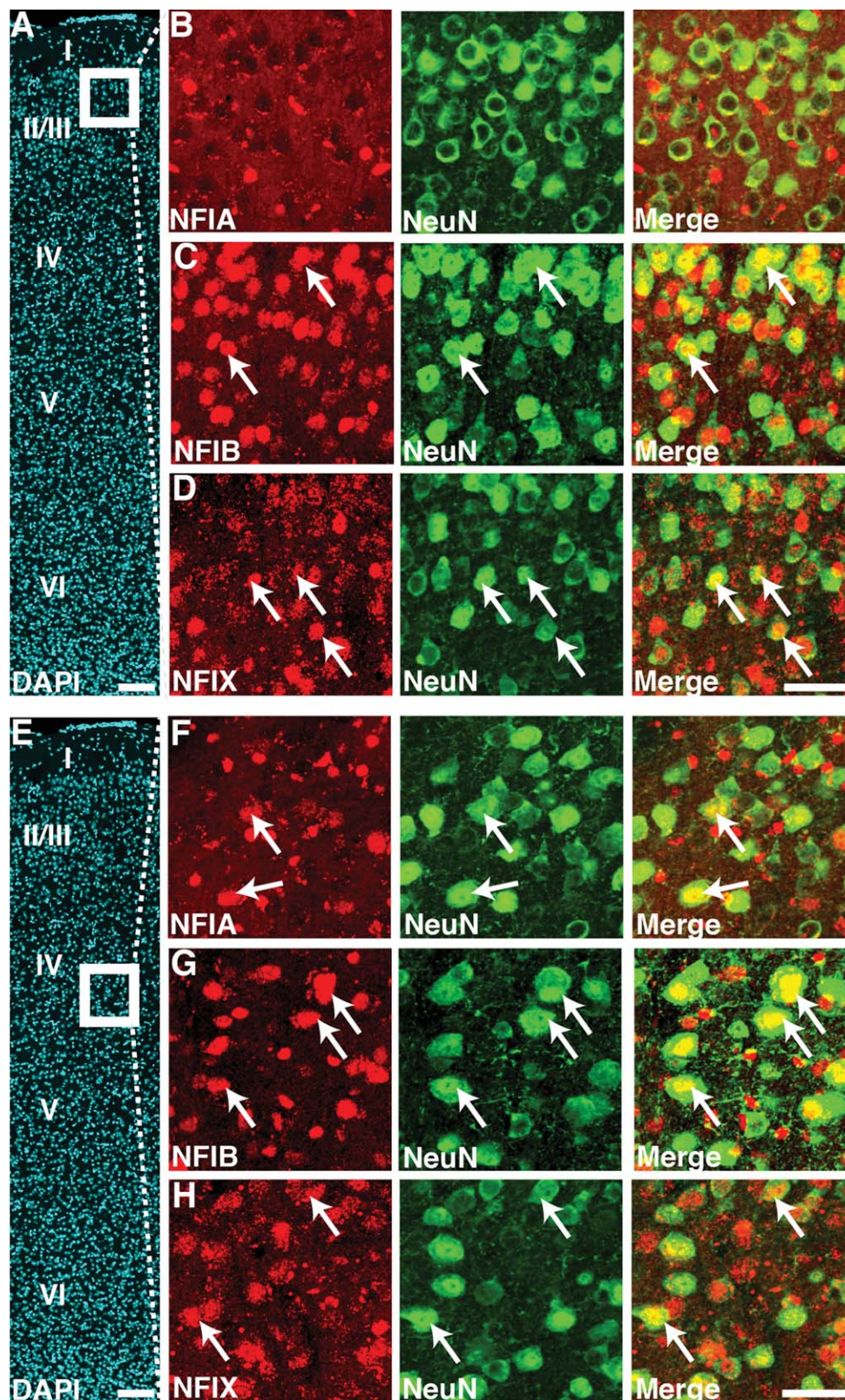


**FIGURE 3** NFI proteins are expressed in neurons in the adult neocortex. The co-expression of NFIA, NFIB, and NFIX proteins with NeuN was examined with immunofluorescence staining in 40  $\mu$ m midline sagittal vibratome sections of adult mouse brains ( $n = 3$  or 4) and imaged on a spinning-disk confocal microscope. (a–l) Co-expression with NeuN was detected for all three NFI proteins in all layers (arrows). The boxed regions represent the higher magnification region that was quantified for each section: (b–d) for top region in (a); (f–h) for middle region in (e); (j–l) for bottom region in (i). The Roman numerals I, II/III, IV, V, and VI denote the respective cortical layers. ROI = region of interest. Scale bars = 100  $\mu$ m in (a), (e), and (i); 50  $\mu$ m in (d) for (b–d); 50  $\mu$ m in (h) for (f–h); 50  $\mu$ m in (l) for (j–l). [Color figure can be viewed at [wileyonlinelibrary.com](http://wileyonlinelibrary.com)]



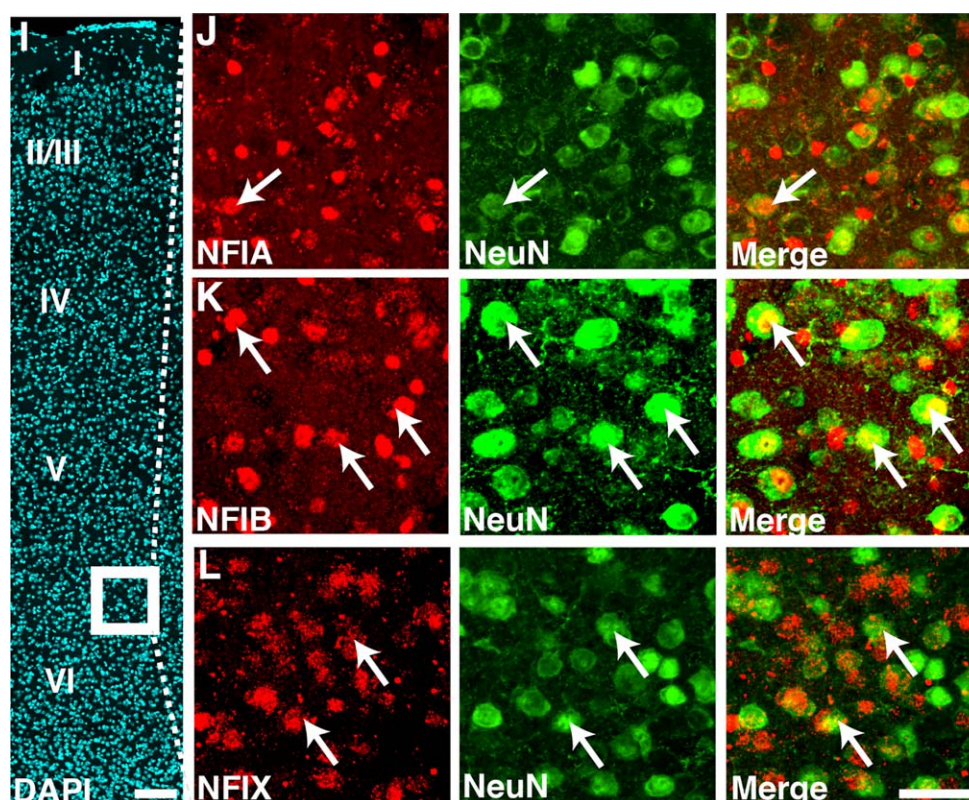


FIGURE 3 Continued.

#### 2.4.2 | Fluorescence IHC

Fluorescence IHC was conducted as previously described with minor modifications (Plachez et al., 2008). The brain sections were antigen-retrieved as for chromogenic IHC. The sections were then incubated for 2 hr in blocking solution containing 10% v/v normal donkey serum, 0.9% v/v  $H_2O_2$ , and 0.2% v/v Triton X-100 in PBS. The sections were incubated overnight with primary antibody diluted in 2% v/v normal donkey serum and 0.2% v/v Triton X-100 in PBS. The primary antibodies are listed in Table 1, with their specificity being confirmed by comparing labeling to IgG secondary antibody control labeling, where immunolabeling was performed under identical conditions with omission of the primary antibody. The sections were washed in PBS for 3x20 min before incubating with the secondary antibody.

For standard fluorescence immunolabeling, donkey anti-rabbit IgG conjugated to Alexa Fluor 488 (Thermo Fisher Scientific, Melbourne, Australia; Cat# A-21206, RRID:AB\_141708) or 555 (Thermo Fisher Scientific; Cat# A-31572, RRID:AB\_16254), donkey anti-mouse IgG conjugated to Alexa Fluor 488 (Thermo Fisher Scientific; Cat# A-21202, RRID:AB\_141607), 555 (1:500; Thermo Fisher Scientific; Cat# A-31570, RRID:AB\_2536180) or 647 (Jackson ImmunoResearch Labs; Cat# 715-606-150, RRID: AB\_2340866), and/or donkey anti-goat IgG conjugated to Alexa Fluor 555 (Thermo Fisher Scientific; Cat# A-21432, RRID:AB\_2535853) were diluted 1:500 in PBS containing 0.2% v/v Triton X-100 and incubated for 3 hr in a humidified light-protected chamber. Alternatively, 1:500 diluted bio-

tinylated donkey anti-rabbit IgG, biotinylated donkey anti-chicken IgY or biotinylated donkey anti-mouse IgG, incubated for 1 hr. The sections were then washed for 3x10 min with PBS before incubation with Streptavidin-Alexa Fluor 647 conjugate (1:500; Thermo Fisher Scientific; Cat# S-21374, RRID:AB\_2336066) diluted in 0.2% Triton X-100 in PBS for 1 hr.

After secondary antibody and amplification incubation, the sections were washed for 3x10 min with PBS and incubated in 4',6-diamidino-2-phenylindole (DAPI) (1 : 1000; Thermo Fisher Scientific; Cat# D1306, RRID:AB\_2629482) in 0.2% Triton X-100 in PBS for 5 min. The sections were then washed for 3x10 min with PBS and coverslipped using ProLong Gold anti-fade reagent (Thermo Fisher Scientific).

#### 2.5 | Image acquisition and analysis

Brightfield imaging was performed with a Zeiss upright Axio-Imager Z2 microscope fitted with a Metasystems-Coolcube1 camera, and captured with VSlide (Metasystems, Boston, US). Fluorescence images were collected using a Marianas spinning-disk confocal system (3I, London, UK) consisting of an Axio Observer Z1 (Carl Zeiss, Jena, Germany) equipped with a CSU-W1 spinning-disk head (Yokogawa Corporation of America, Sugar Land, US), ORCA-Flash 4.0 v2 sCMOS camera (Hamamatsu Photonics, Hamamatsu, Japan), 20x 0.8 NA PlanApo objective, and captured with SlideBook 6.0 (3I). Images were pseudocolored to permit overlay, cropped, sized, and enhanced for contrast and brightness with Photoshop and Illustrator (Adobe



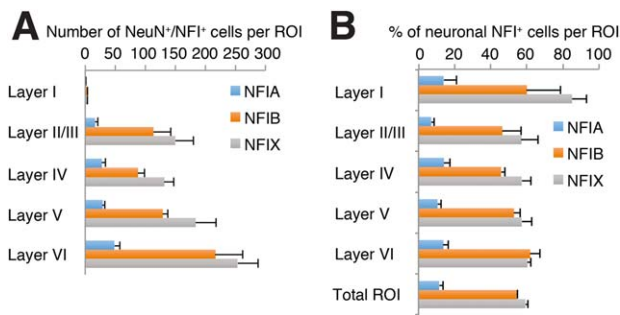


**FIGURE 4** Laminar distribution of NFI-expressing neurons in the adult neocortex. The co-expression of NFIA, NFIB, and NFIX proteins with NeuN in Figure 3 was quantified in a 1,500  $\mu$ m wide ROI for each immunofluorescence-stained brain sections ( $n = 3$  or 4). (a) The total number of NeuN and either NFIA, NFIB, or NFIX co-expressing cells was quantified for each layer in a 1,500  $\mu$ m wide ROI for each section. More double-positive cells were observed in deeper layers than upper layers. (b) The relative distribution of NFI and NeuN double-positive cells was equivalent between layers. [Color figure can be viewed at [wileyonlinelibrary.com](http://wileyonlinelibrary.com)]

Systems, San Jose, CA) or ImageJ (NIH). Automated cell counting of fluorescent images was performed with Imaris 8.2.1 software (Bitplane, Badenerstrasse, Zürich). To minimize sampling biases in the cell type analyses, NFIA, NFIB, and NFIX staining were performed

using separate consecutive 40- $\mu$ m-thick midline sagittal sections, with each section co-stained for a cell type-specific marker and one of the three NFI transcription factors. A 1,500  $\mu$ m wide region of interest (ROI) was identically placed within the neocortex in all sections, and was used for data quantification (Figure 1g). Counts were performed using an unbiased automatic built-in spot detection algorithm in the Imaris software. Positive signals within the ROI with diameter larger than 10  $\mu$ m that colocalize with DAPI were identified as spots or positive counts. A spot colocalization algorithm in the Imaris software was also used to analyze double-labeled cells with a distance threshold value of 6. Two spots were considered colocalized if the distance between the centers of two spots were less or equal to 6  $\mu$ m. Potential false positives were then manually validated by inspection of the overlay signals. The laminar distribution of NFI-NeuN double-labeled cells was determined after sub-dividing the neocortex into its six respective layers. The results of these counts are represented by the mean and SEM, obtained from three or four individual animals (Figure 4a). For all other counts, the results are represented as the mean percentage of positive cells and the standard error of this mean, obtained from counting cells from three or four individual animals. This normalization accounts for cell density, compensating for an initial overcount that may occur, as described previously (Guillery, 2002).

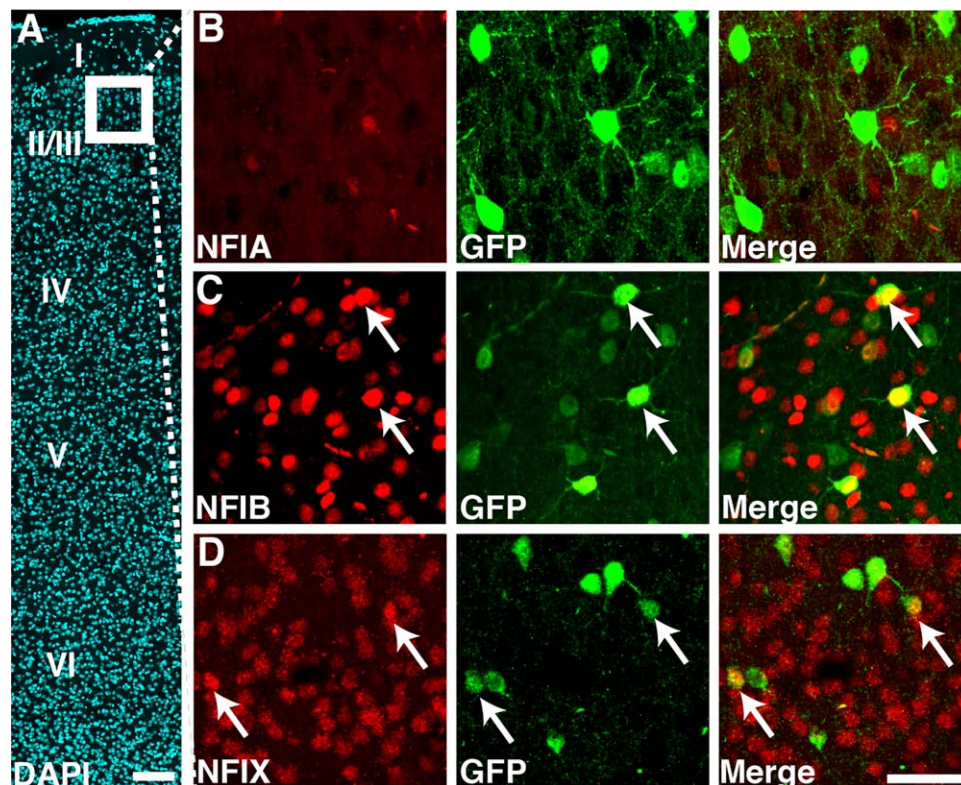


**FIGURE 5** NFIB and NFIX proteins are expressed in GABAergic interneurons in the adult neocortex. The co-expression of NFIA, NFIB, and NFIX proteins with GFP was examined with immunofluorescence staining in 50  $\mu$ m coronal vibratome sections of the adult GAD67-GFP mouse brains and imaged on a spinning-disk confocal microscope. (a–d) Co-expression with GFP was detected only for NFIB and NFIX in GAD67-GFP reporter mouse brain sections. The boxed region in (a) represents the region analyzed in higher magnification images that was obtained from sections in (b–d). The Roman numerals I, II/III, IV, V, and VI denote the respective cortical layers. Scale bars = 100  $\mu$ m in (a); 50  $\mu$ m in (d) for (b–d). [Color figure can be viewed at [wileyonlinelibrary.com](http://wileyonlinelibrary.com)]



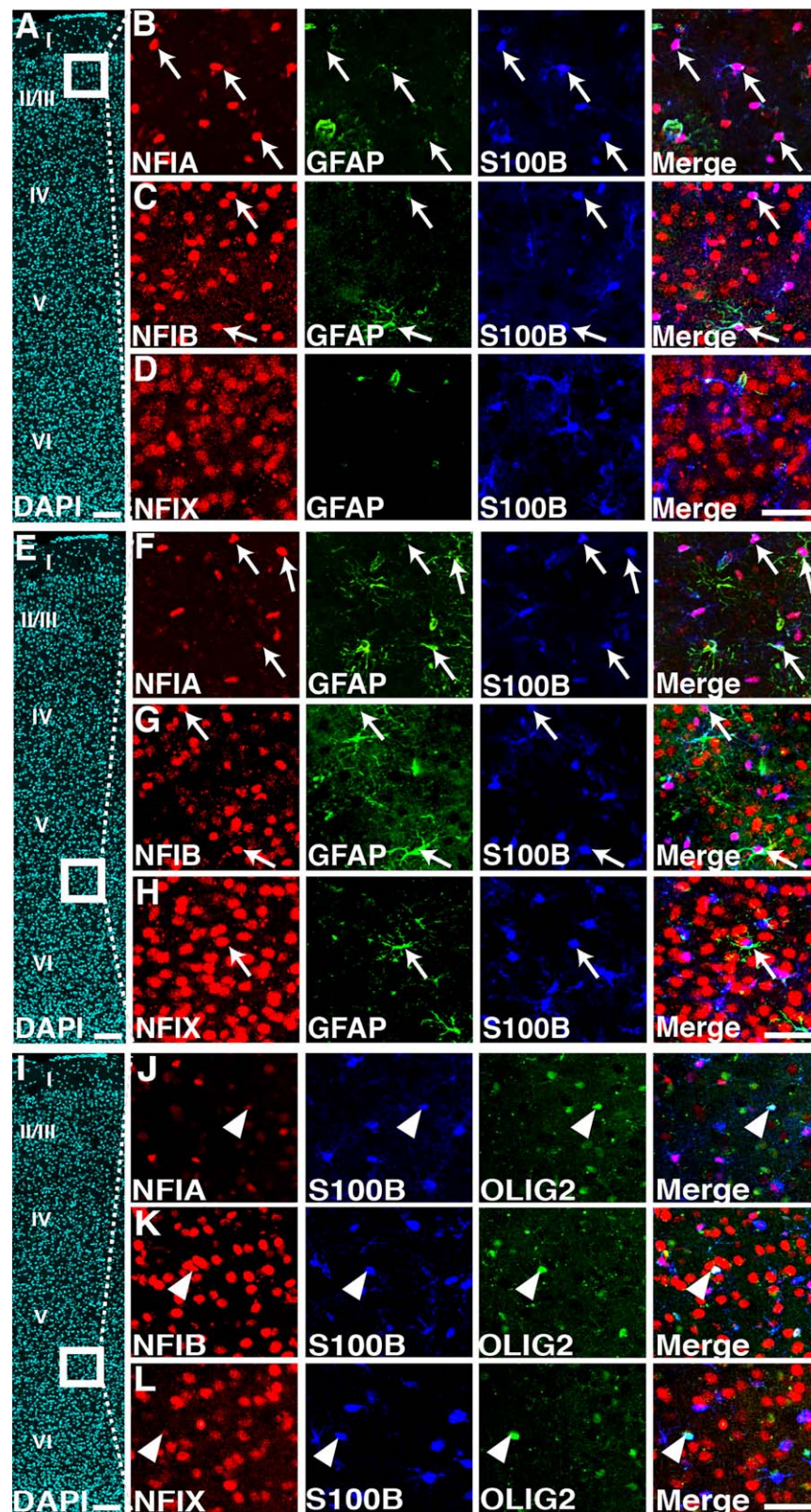


**FIGURE 6** NFI proteins are expressed in astrocytes in the adult neocortex. Immunofluorescence staining was performed on 40  $\mu$ m midline sagittal vibratome sections of adult mouse brains ( $n = 3$  or 4) and imaged on a spinning-disk confocal microscope. (a–h) Co-expression with GFAP and/or S100B was detected for all three NFI proteins in the neocortex (arrows). (i–l) S100B labeled both astrocytes and oligodendroglia, as some S100B-positive cells co-expressed the oligodendrocytic marker OLIG2 (arrowheads). (m) NFIA showed the highest co-expression with astrocytic markers, and NFIX the lowest. The boxed regions represent the higher magnification region that was quantified in consecutive sections for each NFI protein: (b–d) for (a); (f–h) for (e); (j–l) for (i). The Roman numerals I, II/III, IV, V, and VI denote the respective cortical layers. ROI = region of interest. Scale bars = 100  $\mu$ m in (a), (e), and (i); 50  $\mu$ m in (d) for (b–d); 50  $\mu$ m in (h) for (f–h); 50  $\mu$ m in (l) for (j–l). [Color figure can be viewed at [wileyonlinelibrary.com](http://wileyonlinelibrary.com)]



### 3 | RESULTS

#### 3.1 | NFI protein expression shows a distinct laminar distributions in the adult neocortex

To determine the expression pattern of NFIA, NFIB and NFIX in the adult neocortex, 9-month old C57BL/6J mouse brains were sectioned and immunohistochemically stained for each NFI protein (Figure 2). All three family members were expressed throughout the neocortex and cingulate cortex, but their expression patterns differed. In the neocortex, NFIA showed higher expression in layers V and VI as compared to the other layers (Figure 2b,f,j). Similarly, NFIB expression was higher in layers V and VI, followed by the upper region of layer II/III (Figure 2c,g,k). In contrast, NFIX was most highly expressed in layer II/III, followed by layers V and VI (Figure 2d,h,l). These patterns of differential expression across the cortical layers were more pronounced in caudal sections (Figure 2j–l). Expression of all three NFI proteins was also detected in cells located in the corpus callosum and the indusium griseum (arrows in Figure 2n–p). NFIA expression sparsely labeled the cingulate cortex (Figure 2n), whereas NFIB in this region displayed higher expression below the marginal zone (closed arrowhead in Figure 2o) and within the deeper layers (open arrowhead in Figure 2o). NFIX was expressed more uniformly throughout the cingulate cortex, but minimally in the marginal zone (Figure 2p). Together, these data show that although the NFI proteins are broadly expressed throughout the cortex, they are differentially expressed between cortical layers, suggesting that individual NFI proteins might play differing roles across the various populations of cortical neurons.

#### 3.2 | NFI proteins are expressed in neurons in the adult neocortex

To determine whether NFI expression in neurons reflects the distinct laminar distributions observed with chromogenic IHC, co-staining of NFI with the neuronal marker NeuN (Wolf et al., 1996) on midline sagittal sections was performed (Figure 3). Co-expression of the three NFI family members with NeuN was detected throughout the neocortex. The total number of NFI-expressing cells that co-expressed NeuN was lower for NFIA than for NFIB and NFIX within a 1,500  $\mu\text{m}$  wide ROI (Figures 1g and 3a–l). In line with our immunohistochemical data (Figure 2), more NFIA and NeuN co-expressing cells were observed in the deeper cortical layers than in the upper layers (Figures 3b,f,j and 4a). NFIB and NeuN co-expressing cells also approximated to the layered expression pattern observed with chromogenic IHC (Figures 3c,g,k and 4a), whereas co-labeling of NFIX and NeuN was enriched within the deeper layers (Figures 3d,h,l and 4a). Quantification of the number of NFI and NeuN co-labeled cells in each layer demonstrated that NFI-positive neurons occurred in all layers (Figure 4a). When NFI-positive neurons were represented as a percentage of the total NFI-positive cells within each layer, we observed that less than 20% of NFIA-positive cells had a neuronal identity, whereas 50% of all NFIB- or NFIX-positive cells were neurons (Figure 4b).

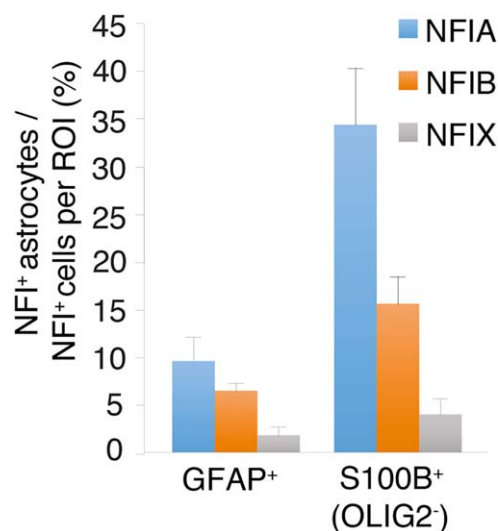


**FIGURE 7** Distribution of NFI-expressing astrocytes in the adult neocortex. The co-expression of NFIA, NFIB, and NFIX proteins with the astrocytic markers GFAP and S100B in Figure 6 was quantified in a 1,500  $\mu\text{m}$  wide ROI for each immunofluorescence-stained brain section ( $n = 3$  or 4). S100B-positive cells that co-expressed OLIG2 were excluded from quantification. NFIA showed the highest co-expression with the astrocytic markers, and NFIX showed the lowest co-expression with these markers. [Color figure can be viewed at [wileyonlinelibrary.com](http://wileyonlinelibrary.com)]

Since NeuN is a pan-neuronal nuclear protein, it does not distinguish between excitatory neurons and inhibitory interneurons (Mullen et al., 1992). To determine whether NFI is expressed in interneurons, we took brain sections from the adult GAD67-GFP reporter mouse and immunolabeled them with GFP as a marker for interneurons. No NFIA and GFP co-expressing cells were detected throughout the neocortex (Figure 5b), whereas co-labeling of NFIB and GFP, as well as NFIX and GFP were observed (Figure 5c,d). We observed that less than 10% of NFIB-positive or NFIX-positive cells in the neocortex were interneurons. This demonstrates that both NFIB and NFIX are expressed in both excitatory neurons and inhibitory interneurons. However, the large proportion of NFI-positive nuclei that did not co-localize with NeuN and GFP suggests that the three NFI proteins are also expressed in non-neuronal cells of the adult neocortex.

#### 3.3 | Astrocytes, oligodendroglia, microglia, and ependymal cells express NFI proteins in the adult neocortex

To assess which other cell types expressed NFI in the adult neocortex, co-staining with markers for astrocytes (S100B, Raponi et al., 2007 and GFAP, Eng, Ghirnikar, & Lee, 2000), oligodendroglia (OLIG2, Ligon et al., 2004), microglia (IBA1, Kanazawa, Ohsawa, Sasaki, Kohsaka, & Imai, 2002), and ependymal cells (FOXJ1, Jacquet et al., 2009) was performed (Figures 5 and 6). Expression of the NFI proteins was detected in both GFAP-positive and S100B-positive astrocytes throughout the neocortex, with GFAP-positive astrocytes observed predominantly

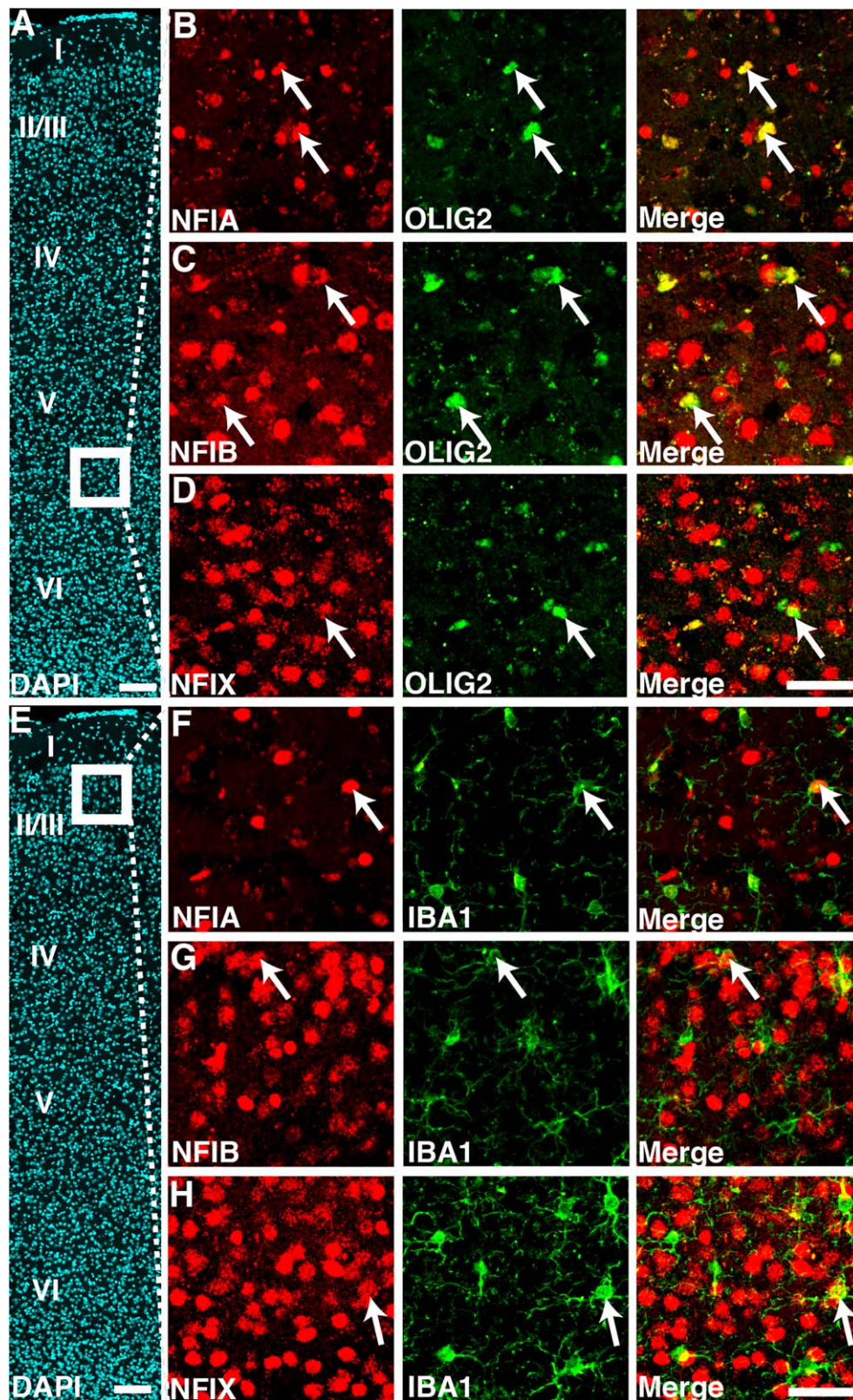


**FIGURE 8** NFI proteins are expressed in oligodendrocytes, microglia, and ependymal cells in the adult neocortex. Immunofluorescence staining was performed on 40  $\mu$ m midline sagittal vibratome sections of adult mouse brains ( $n = 3$  or 4) and imaged on a spinning-disk confocal microscope. (a–d) Co-expression with OLIG2 was detected for the three NFI proteins in the neocortex. (e–h) Co-expression with IBA1 was detected for all three NFI proteins in the neocortex. (i–l) All ependymal cells (FOXJ1+) co-expressed all three NFI proteins in the neocortex. The boxed regions represent the higher magnification region that was quantified in consecutive sections for each NFI protein: (b–d) for (a); (g–i) for (f); (l–n) for (k). The Roman numerals I, II/III, IV, V, and VI denote the respective cortical layers. ROI = region of interest. Scale bars = 100  $\mu$ m in (a), (f), and (k); 50  $\mu$ m in (d) for (b–d); 50  $\mu$ m in (h) for (f–h); 50  $\mu$ m in (l) for (j–l). [Color figure can be viewed at [wileyonlinelibrary.com](http://wileyonlinelibrary.com)]



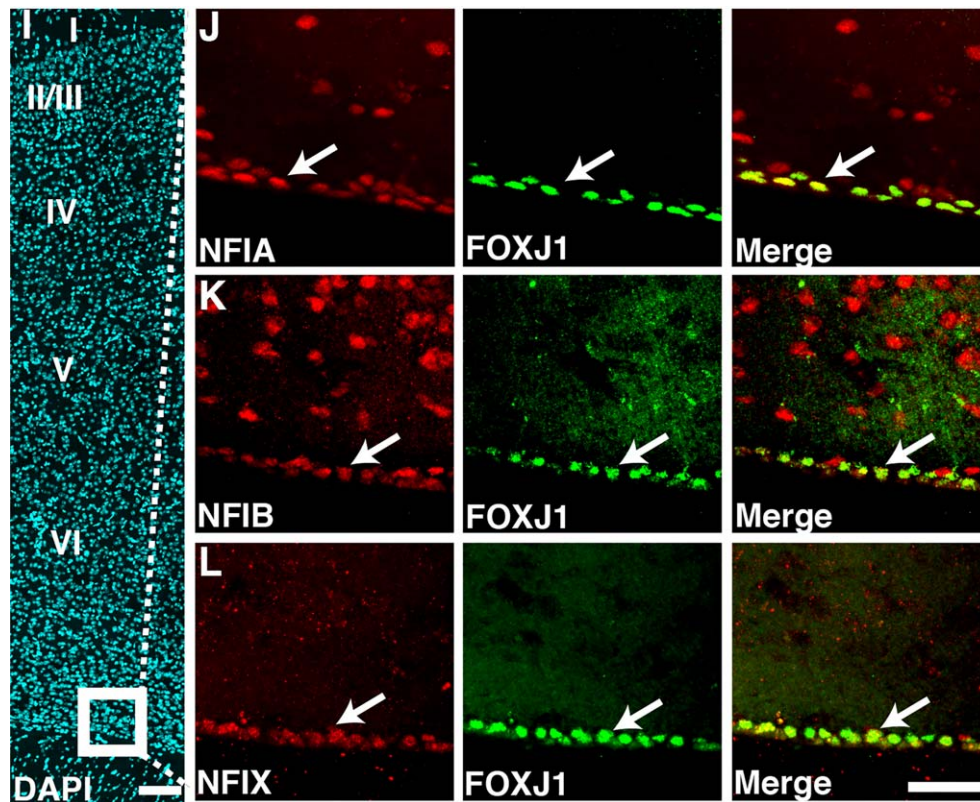


**FIGURE 8** NFI proteins are expressed in oligodendrocytes, microglia, and ependymal cells in the adult neocortex. Immunofluorescence staining was performed on 40  $\mu$ m midline sagittal vibratome sections of adult mouse brains ( $n = 3$  or 4) and imaged on a spinning-disk confocal microscope. (a–d) Co-expression with OLIG2 was detected for the three NFI proteins in the neocortex. (e–h) Co-expression with IBA1 was detected for all three NFI proteins in the neocortex. (i–l) All ependymal cells (FOXJ1+) co-expressed all three NFI proteins in the neocortex. The boxed regions represent the higher magnification region that was quantified in consecutive sections for each NFI protein: (b–d) for (a); (g–i) for (f); (l–n) for (k). The Roman numerals I, II/III, IV, V, and VI denote the respective cortical layers. ROI = region of interest. Scale bars = 100  $\mu$ m in (a), (f), and (k); 50  $\mu$ m in (d) for (b–d); 50  $\mu$ m in (h) for (f–h); 50  $\mu$ m in (l) for (j–l). [Color figure can be viewed at [wileyonlinelibrary.com](http://wileyonlinelibrary.com)]

within the deeper layers of the neocortex (Figure 6a–h). As S100B is also expressed in the oligodendroglial lineage in the brain (Hachem et al., 2005), co-staining of NFI proteins with S100B and OLIG2 was carried out to discriminate oligodendroglia from astrocytes (Figure 6i–l). Approximately 15% of NFIA-expressing cells co-labeled with GFAP, whereas in the case of NFIB and NFIX 5 and 2% were co-labeled, respectively (Figure 7). Approximately 35% of NFIA-expressing cells co-labeled with S100B (OLIG2-negative), compared to 15% for NFIB and less than 5% for NFIX (Figure 7). The NFI expression pattern was similar for both GFAP and S100B, suggesting that NFI expression is equally distributed between these two astrocyte populations. NFI proteins were also expressed in oligodendroglia (Figure 8a–d), with ~25% of NFIA-positive cells co-expressing OLIG2, compared to 10% for NFIB and NFIX in the ROI (Figure 9a). Similarly, co-expression with IBA1, which labels microglia, was detected for all three NFI proteins (Figure 8e–h). Nevertheless, microglia represented only a small proportion of the total NFI-positive cells in the ROI (Figure 9b). Intriguingly, ependymal cells, identified as FOXJ1-positive cells that were located adjacent to the lateral ventricle, expressed all three NFI proteins (Figure 8i–l).

To determine how the NFI proteins were distributed between the cell types examined, we also calculated the fraction of NFIA-, NFIB-, or

NFIX-positive cells representing each cell type within the same ROI (Figure 10). Neurons predominantly expressed NFIB and NFIX (~60%), whereas NFIA was only expressed in ~10% of these cells. Eighty percentage of S100B-positive astrocytes expressed NFIA and NFIB, but only 10% expressed NFIX. Approximately 60% of GFAP-positive astrocytes expressed NFIA and NFIB, but only 20% expressed NFIX. Oligodendroglia predominantly expressed NFIA (~70%), whereas NFIB was expressed in ~40% and NFIX was expressed in less than 20% of these cells. The three NFI proteins were expressed in similar proportions in microglia (less than 30%), whereas 100% of ependymal cells expressed the three NFI family members. Overall, we observed NFIA, NFIB, and NFIX expression in all cell types, although these proteins were distributed differently between the different cell types.

### 3.4 | NFI proteins are expressed during all stages of neural stem cell differentiation in the dentate gyrus

The adult hippocampus, along with the subventricular zone of the lateral ventricles, are remarkable in that they contain the remaining populations of neural stem and progenitor cells that persist into adulthood. We previously analyzed NFI expression in the neural stem cells of the

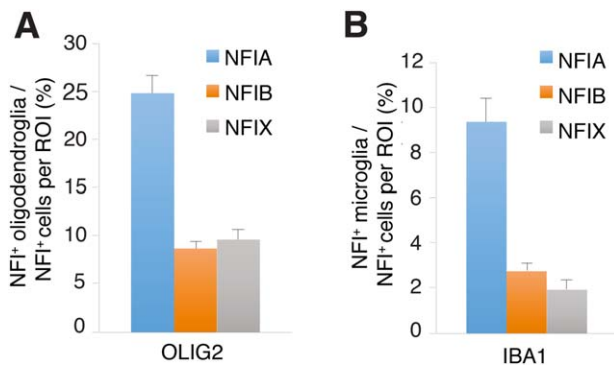


**FIGURE 9** Distribution of NFI-expressing oligodendroglia and microglia in the adult neocortex. The co-expression of NFIA, NFIB, and NFIX proteins with an oligodendroglial (a) and a microglial (b) marker in Figure 8 was quantified in a 1,500  $\mu\text{m}$  wide ROI for each immunofluorescence-stained brain section ( $n = 3$  or 4). (a) Approximately 25% of the NFIA-positive cells were OLIG2-positive, whereas less than 10% of the NFIB- and NFIX-positive populations were OLIG2-positive. (b) Less than 10% of the NFIA-positive population was microglia, whereas this percentage was 3% for NFIB and 2% for NFIX. [Color figure can be viewed at [wileyonlinelibrary.com](http://wileyonlinelibrary.com)]

subventricular zone (Plachez et al., 2008), but their expression in the adult hippocampus had not been examined in detail, despite a known role for NFIX in hippocampal neurogenesis (Martynoga et al., 2013). Specifically, it was recently shown in vitro that NFIX plays a central role in regulating adult neural stem cell quiescence (Martynoga et al., 2013), a process that when disrupted can lead to long-term deficits in hippocampal function (Mira et al., 2010). Immunohistochemical staining for NFI in the adult hippocampus revealed that the three family members were highly expressed in both the pyramidal layer and the dentate gyrus (Figure 11). In the pyramidal layer, NFI expression appeared uni-

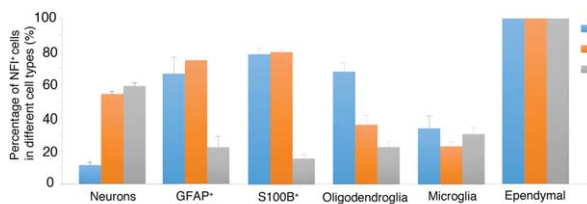


**FIGURE 10** NFI proteins are differently distributed amongst the major cell types of the adult neocortex. Quantification of immunolabeled cells was performed in a 1,500  $\mu\text{m}$  wide ROI of neocortex with separate consecutive 40  $\mu\text{m}$  midline sagittal vibratome sections of the adult mouse brains ( $n = 3$  or 4) for each NFI protein. Approximately 50% of neurons expressed NFIB and/or NFIX, whereas NFIA was expressed in less than 15% of neurons. Approximately 60% of GFAP-positive astrocytes expressed NFIA and NFIB, and only 20% expressed NFIX. Approximately 80% of S100B-positive astrocytes expressed NFIA and NFIB, but less than 10% expressed NFIX. Oligodendroglia predominantly expressed NFIA (~70%), whereas NFIB was expressed in ~40% and NFIX was expressed in less than 20% of these cells. The three NFI proteins were expressed in similar percentages in microglia (20–30%), whereas 100% of ependymal cells expressed all three NFI proteins. [Color figure can be viewed at [wileyonlinelibrary.com](http://wileyonlinelibrary.com)]

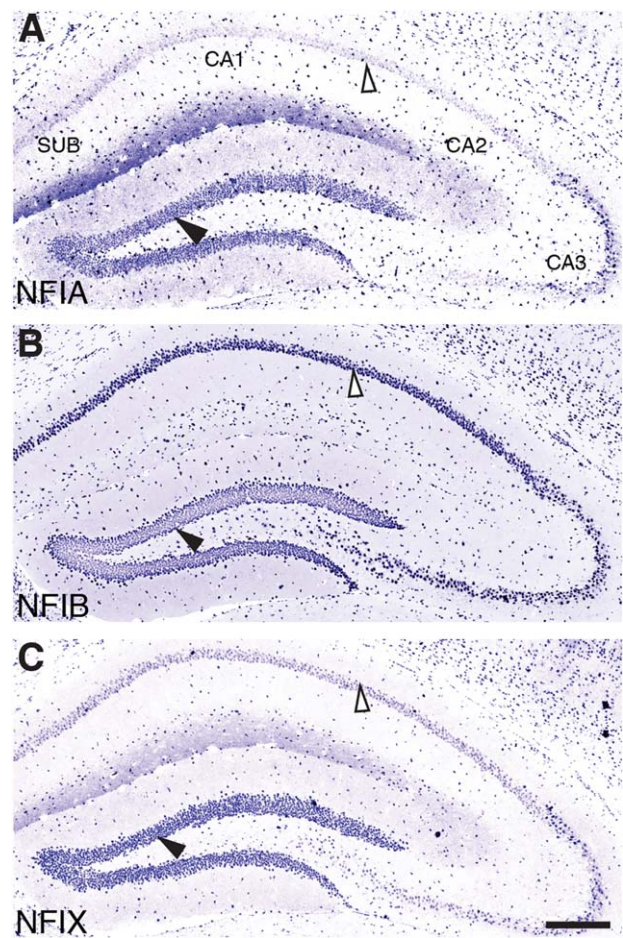


**FIGURE 11** NFI proteins are expressed in the pyramidal layer and dentate gyrus of adult hippocampus. Nickel-DAB immunostaining were performed in 5  $\mu\text{m}$  coronal paraffin-embedded brain sections of adult C57Bl6 wild-type mice ( $n = 6$ ). In the hippocampus, NFI proteins were highly expressed in the pyramidal layer (CA1–CA3 and subiculum) (open arrowhead) and dentate gyrus (closed arrowhead), although NFIA and NFIX expression in pyramidal cells was lower than that of NFIB (a–c). SUB = subiculum. Scale bars = 250  $\mu\text{m}$  in (c) for (a–c). [Color figure can be viewed at [wileyonlinelibrary.com](http://wileyonlinelibrary.com)]

form across the various neuronal compartments, the CA1, CA2, and CA3. Weak staining was observed in the subiculum (Figure 11). Interestingly, the relative expression intensity for NFIA and NFIX was higher in the dentate gyrus than in the pyramidal layer, whereas NFIB expression had the opposite expression profile (Figure 11).

To determine which of the stem and progenitor populations in the dentate gyrus express NFI proteins, co-staining was performed with markers for mature neurons (NeuN), neural progenitors (SOX2, Ellis et al., 2004), neuroblasts (DCX, Brown et al., 2003), and proliferating cells (Ki67, Scholzen & Gerdes, 2000) (Figure 12). All three members of the NFI family were expressed in quiescent SOX2-positive/Ki67-negative Type 1 neural stem cells, and SOX2-positive/Ki67-positive proliferating Type 1 or Type 2 cells (Figure 12a–c). All neuroblasts (DCX-positive) and the majority of dentate granule neurons (NeuN-positive) expressed the three NFI proteins. Interestingly, in contrast to previous



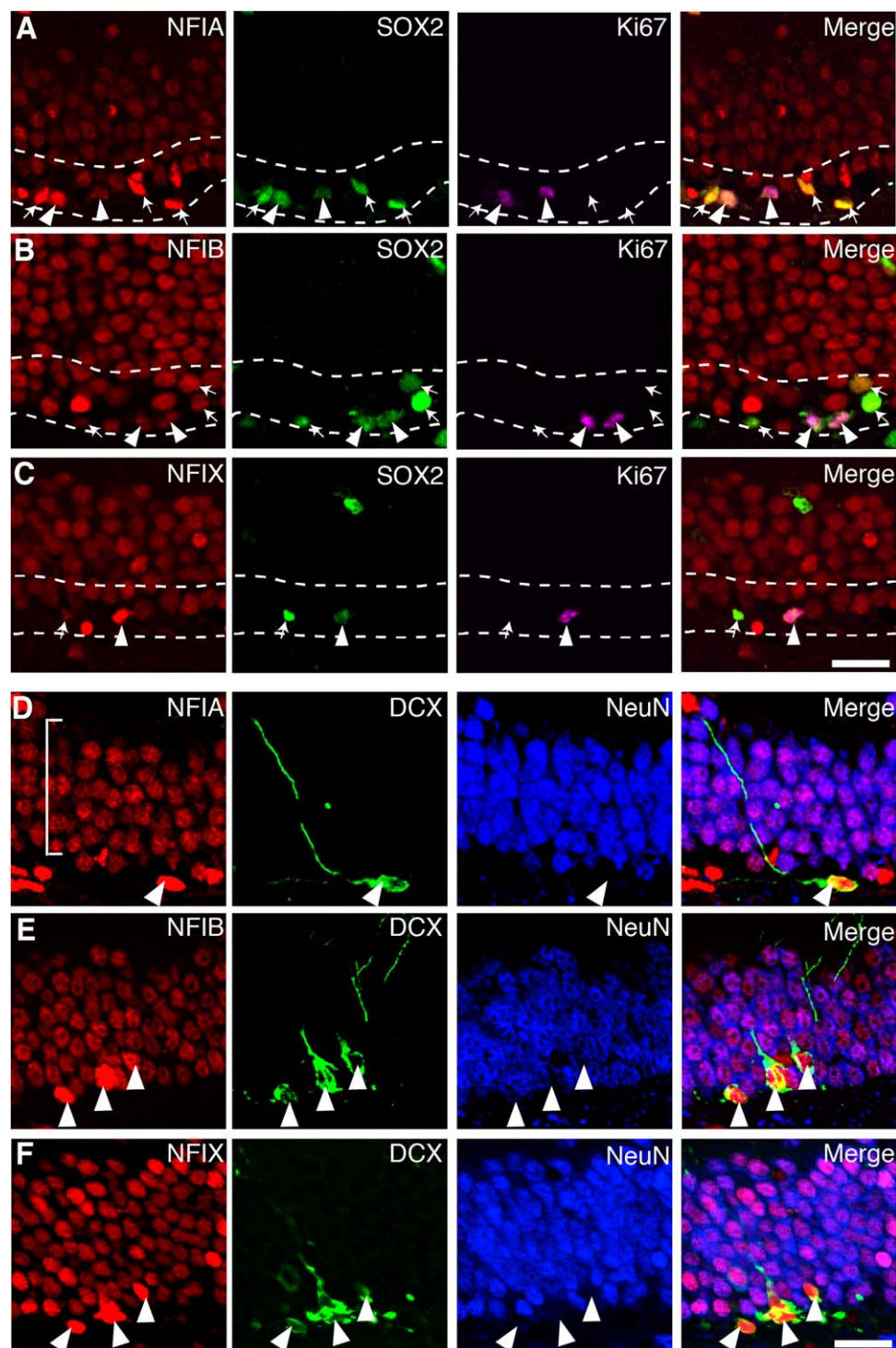


**FIGURE 12** NFI proteins are expressed during all stages of neural stem cell differentiation in the adult dentate gyrus. Immunofluorescence were performed in 5  $\mu$ m coronal paraffin-embedded brain sections of adult C57Bl6 wild-type mice ( $n = 6$ ). Co-expression of the three NFI proteins with SOX2-positive/Ki67-negative cells represented quiescent Type 1 neural stem cells (arrows), whereas co-expression of the three NFI proteins with SOX2-positive/Ki67-positive cells represented proliferating Type 1 neural stem cells or Type 2 intermediate progenitor cells (arrowheads) in the subgranular zone (dashed lines) (a–c). Co-expression of the three NFI proteins with DCX (neuroblast marker) demarcated differentiating neurons (arrowheads), whereas co-expression of the three NFI proteins with NeuN (mature neuronal marker) represented dentate granule neurons (d–f). Note that NFI expression is markedly higher in neuroblasts than in quiescent neural stem cells and immunopositive cells in the granule cell layer (bracket in (d)). The majority of dentate granule neurons (NeuN-positive) expressed NFI proteins. Scale bars = 20  $\mu$ m in (c) for (a–c); 20  $\mu$ m in (f) for (d–f). [Color figure can be viewed at [wileyonlinelibrary.com](http://wileyonlinelibrary.com)]

data in an neural stem cell line (Martynoga et al., 2013), the relative expression intensity of NFI in SOX2-positive/Ki67-positive proliferating cells (Type 1 or Type 2) and in neuroblast cells was more intense than in quiescent stem cells and mature granule neurons (Figure 12d–f). This increased expression of NFI proteins during proliferative stages of adult neurogenesis suggests an important role for NFI in regulating the transition between a progenitor state and neuronal commitment.

## 4 | DISCUSSION

The NFI family of proteins is essential for brain development. A lingering question has been how these genes function after development and whether their function differs between family members. A crucial first step in addressing this issue was to identify whether the proteins are expressed in the adult brain, and if so where and by which cell types, to enable further investigation of their function. In this study, we found that NFIA, NFIB, and NFIX proteins are expressed throughout the adult cerebral cortex. Although distributed differently, these three family members are expressed in all major cell types in this region, including excitatory neurons, inhibitory interneurons, astrocytes, oligodendroglia, microglia, ependymal cells, neural stem cells, and dentate granule neurons. These findings are in line with the detection of *NFIA*, *NFIB*, and *NFIX* mRNA in different postnatal cortical layers and cell types of the cortex in RNA-sequencing data sets (Belgard et al., 2011; Cahoy et al., 2008; Doyle et al., 2008; Zhang et al., 2014). As none of the NFI proteins demarcates a specific cell population, NFI expression cannot be used as a cell type-specific marker (Breunig et al., 2012; Molofsky et al., 2012). However, the differential expression profiles of various family members in different cell types suggests specific biological functions.

The expression patterns of NFI proteins could indicate different roles in cell lineage specification. For instance, NFIA is required for gliogenesis in the spinal cord (Deneen et al., 2006; Glasgow et al., 2014). The co-labeling of astrocytes and oligodendroglia with NFIA in the adult neocortex suggests a similar role in the lineage progression of these cells during postnatal differentiation (Ge, Miyawaki, Gage, Jan, & Jan, 2012; Ivanova et al., 2003). This coincides with mis-regulation of oligodendrocytic genes in the postnatal *Nfia*<sup>-/-</sup> brain (Wong et al., 2007). Intriguingly, our observation that both NFIA and NFIB were expressed in most astrocytes also supports previous data demonstrating that NFIA and NFIB are required to reprogram fibroblasts into astrocytes in vitro (Caiazzo et al., 2015). Hence, NFIB might act as the determining factor for driving astrogliogenesis instead of oligodendrogenesis in the presence of NFIA.

In contrast, our data also show that the majority of excitatory and inhibitory neurons in the adult neocortex express NFIB and NFIX, whereas less than 10% of excitatory neurons and no interneurons express NFIA (Figure 4). This finding suggests that the combined expression of NFIB and NFIX might be more important for neurogenic lineage specification. The loss of NFIX has previously been shown to enhance the lineage progression of oligodendrocytes from neural stem cells in vitro (Zhou et al., 2015). It would be interesting to determine

whether NFIA expression is causal in driving enhanced oligodendrogenesis following *Nfix* deletion. Our data suggest that the ratio of expression levels of multiple family members per cell, rather than individual expression, might be more important for cell lineage specification. Further studies using conditional gene inactivation mouse models and co-staining of the different family members during lineage progression of different cell types are required to further understand the importance of NFI proteins in cell lineage specification.

In addition, the expression of NFIX was also previously reported to be robustly induced to drive and maintaining the quiescence of neural stem cells in vitro, whereas NFIA and NFIB expression were downregulated or unchanged (Martynoga et al., 2013). Here, we found that NFIA, NFIB, and NFIX are all robustly induced during proliferation and differentiation in the adult dentate gyrus, suggesting that all NFI genes are involved in neuronal differentiation and specification in vivo. However, functional in vivo studies, where NFI proteins are selectively deleted from neural stem cells, progenitors, and neuroblasts will be required to clarify this.

Apart from cell lineage specification, NFI proteins could be important for the maintenance of cell identity in the adult brain, as the expression of these proteins persists in adulthood. Whether NFI proteins are required for other functions also remains to be determined. For example, it has been suggested that NFIA is involved in the neuroprotection of neurons following administration of sub-lethal doses of N-methyl-D-aspartate (Zheng et al., 2010) and inhibition of remyelination in human myelin disorders via regulation of oligodendrocyte progenitor differentiation (Fancy et al., 2012). NFI proteins have also been implicated in mental disorders, such as autism (Chuang et al., 2015; Tsang et al., 2013) and bipolar disorder (Le-Niculescu et al., 2009), as well as multiple sclerosis (Fancy et al., 2012), Parkinson's disease (Suwarnalata et al., 2016), and brain tumours (Genovesi et al., 2013; Glasgow et al., 2013; Ho et al., 2013; Idbaih et al., 2008; Lacroix et al., 2014; Lastowska et al., 2013; Lee et al., 2014; Song et al., 2010; Stringer et al., 2016; Vyazunova et al., 2014). The NFI expression pattern in the adult cortex provides a basis for investigating their function in these diseases, and identifying the cell types involved. For instance, NFIA (Glasgow et al., 2013; Lee et al., 2014; Song et al., 2010; Vyazunova et al., 2014) and NFIB (Idbaih et al., 2008; Stringer et al., 2016) are both associated with the progression of glioma, a brain cancer of astrocytic origin. Future studies using cell type-specific and/or inducible deletion of NFI proteins will be required to delineate their precise role in these cell types in order to understand the full extent of their post-developmental role. Our study provides a baseline from which to understand the emerging role of these proteins in brain diseases and their involvement in cell lineage specification and maintenance in the adult brain.

## ACKNOWLEDGMENTS

We would like to thank the staff of the University of Queensland Biological Resources (UQBR) animal facility, Robert Sullivan of the Histology Facility, and Luke Hammond of the Advanced Microscopy Facility at the Queensland Brain Institute for their expertise. We



thank Rowan Tweedale for her critical comments on the manuscript and the laboratory of Pankaj Sah at the Queensland Brain Institute for providing the GAD67-GFP brain tissues.

### CONFLICT OF INTEREST STATEMENT

The authors declare no conflicts of interest.

### ROLE OF AUTHORS

All authors had full access to all the data in the study and take responsibility for the integrity of the data and the accuracy of the data analysis. Study concept and design: KSC, JB, LJR, MP, LH. Acquisition of data: KSC, LH. Analysis and interpretation of data: KSC, JB, LH. Drafting of the manuscript: KSC, JB, LH. Critical revision of the manuscript for important intellectual content: JWCL, MP, LJR, RMG. Administrative, technical, and material support: TJH. Statistical analysis: KSC, JB. Obtained funding: JB, LJR, MP. Study supervision: JB, LJR.

### REFERENCES

- Barry, G., Piper, M., Lindwall, C., Moldrich, R., Mason, S., Little, E., ... Richards, L. J. (2008). Specific glial populations regulate hippocampal morphogenesis. *Journal of Neuroscience*, 28, 12328–12340.
- Belgard, T. G., Marques, A. C., Oliver, P. L., Abaan, H. O., Sirey, T. M., Hoerder-Suabedissen, A., ... Ponting, C. P. (2011). A transcriptomic atlas of mouse neocortical layers. *Neuron*, 71, 605–616.
- Betancourt, J., Katzman, S., & Chen, B. (2014). Nuclear factor one B regulates neural stem cell differentiation and axonal projection of corticofugal neurons. *Journal of Comparative Neurology*, 522, 6–35.
- Bloch, J., Kaeser, M., Sadeghi, Y., Rouiller, E. M., Redmond Jr., D. E., & Brunet, J. F. (2011). Doublecortin-positive cells in the adult primate cerebral cortex and possible role in brain plasticity and development. *Journal of Comparative Neurology*, 519, 775–789.
- Breunig, J. J., Gate, D., Levy, R., Rodriguez Jr., J., Kim, G. B., Danielpour, M., ... Town, T. (2012). Rapid genetic targeting of pial surface neural progenitors and immature neurons by neonatal electroporation. *Neural Development*, 7, 26.
- Brown, J. P., Couillard-Despres, S., Cooper-Kuhn, C. M., Winkler, J., Aigner, L., & Kuhn, H. G. (2003). Transient expression of doublecortin during adult neurogenesis. *Journal of Comparative Neurology*, 467, 1–10.
- Bunt, J., Lim, J. W., Zhao, L., Mason, S., & Richards, L. J. (2015). PAX6 does not regulate Nfia and Nfib expression during neocortical development. *Scientific Reports*, 5, 10668.
- Cahoy, J. D., Emery, B., Kaushal, A., Foo, L. C., Zamanian, J. L., Christopherson, K. S., ... Barres, B. A. (2008). A transcriptome database for astrocytes, neurons, and oligodendrocytes: A new resource for understanding brain development and function. *Journal of Neuroscience*, 28, 264–278.
- Caiazzo, M., Giannelli, S., Valente, P., Lignani, G., Carissimo, A., Sessa, A., ... Broccoli, V. (2015). Direct conversion of fibroblasts into functional astrocytes by defined transcription factors. *Stem Cell Reports*, 4, 25–36.
- Campbell, C. E., Piper, M., Plachez, C., Yeh, Y. T., Baizer, J. S., Osinski, J. M., ... Gronostajski, R. M. (2008). The transcription factor Nfix is essential for normal brain development. *BMC Developmental Biology*, 8, 52.
- Chaudhry, A. Z., Lyons, G. E., & Gronostajski, R. M. (1997). Expression patterns of the four nuclear factor I genes during mouse embryogenesis indicate a potential role in development. *Developmental Dynamics*, 208, 313–325.
- Chuang, H. C., Huang, T. N., & Hsueh, Y. P. (2015). T-Brain-1—a potential master regulator in autism spectrum disorders. *Autism Research*, 8, 412–426.
- Clase, A. C., Dimcheff, D. E., Favara, C., Dorward, D., McAtee, F. J., Parrie, L. E., ... Portis, J. L. (2006). Oligodendrocytes are a major target of the toxicity of spongiform murine retroviruses. *American Journal of Pathology*, 169, 1026–1038.
- das Neves, L., Duchala, C. S., Tolentino-Silva, F., Haxhiu, M. A., Colmeares, C., Macklin, W. B., ... Gronostajski, R. M. (1999). Disruption of the murine nuclear factor I-A gene (Nfia) results in perinatal lethality, hydrocephalus, and agenesis of the corpus callosum. *Proceedings of the National Academy of Sciences of the United States of America*, 96, 11946–11951.
- Deneen, B., Ho, R., Lukaszewicz, A., Hochstim, C. J., Gronostajski, R. M., & Anderson, D. J. (2006). The transcription factor NFIA controls the onset of gliogenesis in the developing spinal cord. *Neuron*, 52, 953–968.
- Desfeux, A., El Ghazi, F., Jegou, S., Legros, H., Marret, S., L Audenbach, V., & Gonzalez, B. J. (2010). Dual effect of glutamate on GABAergic interneuron survival during cerebral cortex development in mice neonates. *Cerebral Cortex*, 20, 1092–1108.
- Doyle, J. P., Dougherty, J. D., Heiman, M., Schmidt, E. F., Stevens, T. R., Ma, G., ... Heintz, N. (2008). Application of a translational profiling approach for the comparative analysis of CNS cell types. *Cell*, 135, 749–762.
- Driller, K., Pagenstecher, A., Uhl, M., Omran, H., Berlis, A., Grunder, A., & Sippel, A. E. (2007). Nuclear factor I X deficiency causes brain malformation and severe skeletal defects. *Molecular and Cellular Biology*, 27, 3855–3867.
- Ellis, P., Fagan, B. M., Magness, S. T., Hutton, S., Taranova, O., Hayashi, S., ... Pevny, L. (2004). SOX2, a persistent marker for multipotential neural stem cells derived from embryonic stem cells, the embryo or the adult. *Developmental Neuroscience*, 26, 148–165.
- Eng, L. F., & Ghirnikar, R. S. (1994). GFAP and astrogliosis. *Brain Pathology*, 4, 229–237.
- Eng, L. F., Ghirnikar, R. S., & Lee, Y. L. (2000). Glial fibrillary acidic protein: GFAP-thirty-one years (1969–2000). *Neurochemical Research*, 25, 1439–1451.
- Fancy, S. P., Glasgow, S. M., Finley, M., Rowitch, D. H., & Deneen, B. (2012). Evidence that nuclear factor IA inhibits repair after white matter injury. *Annals of Neurology*, 72, 224–233.
- Ferri, A. L., Cavallaro, M., Braidia, D., Di Cristofano, A., Canta, A., Vezzani, A., ... Nicolis, S. K. (2004). Sox2 deficiency causes neurodegeneration and impaired neurogenesis in the adult mouse brain. *Development*, 131, 3805–3819.
- Franklin, K. B., & Paxinos, G. (1997). The mouse brain in stereotaxic coordinates. San Diego: Academic Press.
- Ge, W. P., Miyawaki, A., Gage, F. H., Jan, Y. N., & Jan, L. Y. (2012). Local generation of glia is a major astrocyte source in postnatal cortex. *Nature*, 484, 376–380.
- Genovesi, L. A., Ng, C. G., Davis, M. J., Remke, M., Taylor, M. D., Adams, D. J., ... Wainwright, B. J. (2013). Sleeping Beauty mutagenesis in a mouse medulloblastoma model defines networks that discriminate between human molecular subgroups. *Proceedings of the National Academy of Sciences of the United States of America*, 110, E4325–4334.

- Glasgow, S. M., Laug, D., Brawley, V. S., Zhang, Z., Corder, A., Yin, Z., ... Deneen, B. (2013). The miR-223/nuclear factor I-A axis regulates glial precursor proliferation and tumorigenesis in the CNS. *Journal of Neuroscience*, 33, 13560–13568.
- Glasgow, S. M., Zhu, W., Stolt, C. C., Huang, T. W., Chen, F., LoTurco, J. J., ... Deneen, B. (2014). Mutual antagonism between Sox10 and NFIA regulates diversification of glial lineages and glioma subtypes. *Nature Neuroscience*, 17, 1322–1329.
- Grimm, P. R., Foutz, R. M., Brenner, R., & Sansom, S. C. (2007). Identification and localization of BK-beta subunits in the distal nephron of the mouse kidney. *American journal of physiology. Renal physiology*, 293, F350–F359.
- Guillery, R. W. (2002). On counting and counting errors. *Journal of Comparative Neurology*, 447, 1–7.
- Hachem, S., Aguirre, A., Vives, V., Marks, A., Gallo, V., & Legraverend, C. (2005). Spatial and temporal expression of S100B in cells of oligodendrocyte lineage. *Glia*, 51, 81–97.
- Harris, L., Dixon, C., Cato, K., Heng, Y. H., Kurniawan, N. D., Ullmann, J. F., ... Piper, M. (2013). Heterozygosity for nuclear factor one x affects hippocampal-dependent behaviour in mice. *PLoS One*, 8, e65478.
- Harris, L., Genovesi, L. A., Gronostajski, R. M., Wainwright, B. J., & Piper, M. (2015). Nuclear factor one transcription factors: Divergent functions in developmental versus adult stem cell populations. *Developmental Dynamics*, 244, 227–238.
- Heng, Y. H., McLeay, R. C., Harvey, T. J., Smith, A. G., Barry, G., Cato, K., ... Piper, M. (2014). NFIX regulates neural progenitor cell differentiation during hippocampal morphogenesis. *Cerebral Cortex*, 24, 261–279.
- Heng, Y. H., Zhou, B., Harris, L., Harvey, T., Smith, A., Horne, E., ... Piper, M. (2015). NFIX regulates proliferation and migration within the murine SVZ neurogenic niche. *Cerebral Cortex*, 25, 3758–3778.
- Ho, C. Y., Bar, E., Giannini, C., Marchionni, L., Karajannis, M. A., Zagzag, D., ... Rodriguez, F. J. (2013). MicroRNA profiling in pediatric pilocytic astrocytoma reveals biologically relevant targets, including PBX3, NFIB, and METAP2. *Neuro-Oncology*, 15, 69–82.
- Idbaih, A., Carvalho Silva, R., Criniere, E., Marie, Y., Carpentier, C., Boisselier, B., ... Delattre, J. Y. (2008). Genomic changes in progression of low-grade gliomas. *Journal of Neuro-Oncology*, 90, 133–140.
- Ito, D., Imai, Y., Ohsawa, K., Nakajima, K., Fukuuchi, Y., & Kohsaka, S. (1998). Microglia-specific localisation of a novel calcium binding protein, Iba1. *Brain research. Molecular brain research*, 57, 1–9.
- Ivanova, A., Nakahira, E., Kagawa, T., Oba, A., Wada, T., Takebayashi, H., ... Ikenaka, K. (2003). Evidence for a second wave of oligodendrogenesis in the postnatal cerebral cortex of the mouse. *Journal of Neuroscience Research*, 73, 581–592.
- Jacquet, B. V., Salinas-Mondragon, R., Liang, H., Therit, B., Buie, J. D., Dykstra, M., ... Ghashghaei, H. T. (2009). FoxJ1-dependent gene expression is required for differentiation of radial glia into ependymal cells and a subset of astrocytes in the postnatal brain. *Development*, 136, 4021–4031.
- Jezela-Stanek, A., Kucharczyk, M., Falana, K., Jurkiewicz, D., Mlynec, M., Wicher, D., ... Krajewska-Walasek, M. (2016). Malan syndrome (Sotos syndrome 2) in two patients with 19p13.2 deletion encompassing NFIX gene and novel NFIX sequence variant. *Biomedical papers of the Medical Faculty of the University Palacký, Olomouc, Czechoslovakia*, 160, 161–167.
- Ji, J., Salamon, N., & Quintero-Rivera, F. (2014). Microdeletion of 1p32-p31 involving NFIA in a patient with hypoplastic corpus callosum, ventriculomegaly, seizures and urinary tract defects. *European Journal of Medical Genetics*, 57, 267–268.
- Jordan, F. L., Rieke, G. K., Hughes, B. W., & Thomas, W. E. (1990). Morphological diversity of ependymal cells in tissue culture. *Brain Research Bulletin*, 25, 159–163.
- Kalm, M., Lannering, B., Bjork-Eriksson, T., & Blomgren, K. (2009). Irradiation-induced loss of microglia in the young brain. *Journal of Neuroimmunology*, 206, 70–75.
- Kanazawa, H., Ohsawa, K., Sasaki, Y., Kohsaka, S., & Imai, Y. (2002). Macrophage/microglia-specific protein Iba1 enhances membrane ruffling and Rac activation via phospholipase C-gamma -dependent pathway. *The Journal of Biological Chemistry*, 277, 20026–20032.
- Lacroix, J., Schlund, F., Leuchs, B., Adolph, K., Sturm, D., Bender, S., ... Witt, H. (2014). Oncolytic effects of parvovirus H-1 in medulloblastoma are associated with repression of master regulators of early neurogenesis. *International Journal of Cancer*, 134, 703–716.
- Lastowska, M., Al-Afghani, H., Al-Balool, H. H., Sheth, H., Mercer, E., Coxhead, J. M., ... Jackson, M. S. (2013). Identification of a neuronal transcription factor network involved in medulloblastoma development. *Acta Neuropathologica Communications*, 1, 35.
- Le-Niculescu, H., Patel, S. D., Bhat, M., Kuczenski, R., Faraone, S. V., Tsuang, M. T., ... Niculescu 3rd, A. B. (2009). Convergent functional genomics of genome-wide association data for bipolar disorder: Comprehensive identification of candidate genes, pathways and mechanisms. *American Journal of Medical Genetics Part B: Neuropsychiatric Genetics*, 150B, 155–181.
- Lee, J. S., Xiao, J., Patel, P., Schade, J., Wang, J., Deneen, B., ... Song, H. R. (2014). A novel tumor-promoting role for nuclear factor IA in glioblastomas is mediated through negative regulation of p53, p21, and PAI1. *Neuro-Oncology*, 16, 191–203.
- Ligon, K. L., Alberta, J. A., Kho, A. T., Weiss, J., Kwaan, M. R., Nutt, C. L., ... Rowitch, D. H. (2004). The oligodendroglial lineage marker OLIG2 is universally expressed in diffuse gliomas. *Journal of Neuropathology & Experimental Neurology*, 63, 499–509.
- Lu, W., Quintero-Rivera, F., Fan, Y., Alkuraya, F. S., Donovan, D. J., Xi, Q., ... Maas, R. L. (2007). NFIA haploinsufficiency is associated with a CNS malformation syndrome and urinary tract defects. *PLoS Genetics*, 3, e80.
- Malan, V., Rajan, D., Thomas, S., Shaw, A. C., Louis Dit Picard, H., Layet, V., ... Cormier-Daire, V. (2010). Distinct effects of allelic NFIX mutations on nonsense-mediated mRNA decay engender either a Sotos-like or a Marshall-Smith syndrome. *American Journal of Human Genetics*, 87, 189–198.
- Martynoga, B., Mateo, J. L., Zhou, B., Andersen, J., Achimastou, A., Urban, N., ... Guillemot, F. (2013). Epigenomic enhancer annotation reveals a key role for NFIX in neural stem cell quiescence. *Genes & Development*, 27, 1769–1786.
- Mira, H., Andreu, Z., Suh, H., Lie, D. C., Jessberger, S., Consiglio, A., ... Gage, F. H. (2010). Signaling through BMPRII regulates quiescence and long-term activity of neural stem cells in the adult hippocampus. *Cell Stem Cell*, 7, 78–89.
- Molofsky, A. V., Krencik, R., Ullian, E. M., Tsai, H. H., Deneen, B., Richardson, W. D., ... Rowitch, D. H. (2012). Astrocytes and disease: A neurodevelopmental perspective. *Genes & Development*, 26, 891–907.
- Mullen, R. J., Buck, C. R., & Smith, A. M. (1992). NeuN, a neuronal specific nuclear protein in vertebrates. *Development*, 116, 201–211.
- Muller, A., Stellmacher, A., Freitag, C. E., Landgraf, P., & Dieterich, D. C. (2015). Monitoring astrocytic proteome dynamics by cell type-specific protein labeling. *PLoS One*, 10, e0145451.
- Nagao, M., Ogata, T., Sawada, Y., & Gotoh, Y. (2016). Zbtb20 promotes astrocytogenesis during neocortical development. *Nature Communications*, 7, 11102.



- Nyboe, D., Kreiborg, S., Kirchhoff, M., & Hove, H. B. (2015). Familial craniosynostosis associated with a microdeletion involving the NFIA gene. *Clinical Dysmorphology*, 24, 109–112.
- Parkhurst, C. N., Yang, G., Ninan, I., Savas, J. N., Yates 3rd, J. R., Lafaille, J. J., ... Gan, W. B. (2013). Microglia promote learning-dependent synapse formation through brain-derived neurotrophic factor. *Cell*, 155, 1596–1609.
- Pecchi, E., Dallaporta, M., Charrier, C., Pio, J., Jean, A., Moyse, E., & Trodec, J. D. (2007). Glial fibrillary acidic protein (GFAP)-positive radial-like cells are present in the vicinity of proliferative progenitors in the nucleus tractus solitarius of adult rat. *Journal of Comparative Neurology*, 501, 353–368.
- Piper, M., Barry, G., Harvey, T. J., McLeay, R., Smith, A. G., Harris, L., ... Richards, L. J. (2014). NFIB-mediated repression of the epigenetic factor Ezh2 regulates cortical development. *Journal of Neuroscience*, 34, 2921–2930.
- Piper, M., Barry, G., Hawkins, J., Mason, S., Lindwall, C., Little, E., ... Richards, L. J. (2010). NFIA controls telencephalic progenitor cell differentiation through repression of the Notch effector Hes1. *Journal of Neuroscience*, 30, 9127–9139.
- Piper, M., Harris, L., Barry, G., Heng, Y. H., Plachez, C., Gronostajski, R. M., & Richards, L. J. (2011). Nuclear factor one X regulates the development of multiple cellular populations in the postnatal cerebellum. *Journal of Comparative Neurology*, 519, 3532–3548.
- Piper, M., Moldrich, R. X., Lindwall, C., Little, E., Barry, G., Mason, S., ... Richards, L. J. (2009). Multiple non-cell-autonomous defects underlie neocortical callosal dysgenesis in Nfib-deficient mice. *Neural Development*, 4, 43.
- Plachez, C., Cato, K., McLeay, R. C., Heng, Y. H., Bailey, T. L., Gronostajski, R. M., ... Piper, M. (2012). Expression of nuclear factor one A and -B in the olfactory bulb. *Journal of Comparative Neurology*, 520, 3135–3149.
- Plachez, C., Lindwall, C., Sunn, N., Piper, M., Moldrich, R. X., Campbell, C. E., ... Richards, L. J. (2008). Nuclear factor I gene expression in the developing forebrain. *Journal of Comparative Neurology*, 508, 385–401.
- Priolo, M., Grosso, E., Mammi, C., Labate, C., Naretto, V. G., Vacalebri, C., ... Lagana, C. (2012). A peculiar mutation in the DNA-binding/dimerization domain of NFIX causes Sotos-like overgrowth syndrome: A new case. *Gene*, 511, 103–105.
- Raponi, E., Agenes, F., Delphin, C., Assard, N., Baudier, J., Legraverend, C., & Deloulme, J. C. (2007). S100B expression defines a state in which GFAP-expressing cells lose their neural stem cell potential and acquire a more mature developmental stage. *Glia*, 55, 165–177.
- Sajan, S. A., Fernandez, L., Nieh, S. E., Rider, E., Bukshpun, P., Wakahiro, M., ... Sherr, E. H. (2013). Both rare and de novo copy number variants are prevalent in agenesis of the corpus callosum but not in cerebellar hypoplasia or polymicrogyria. *PLoS Genetics*, 9, e1003823.
- Scholzen, T., & Gerdes, J. (2000). The Ki-67 protein: From the known and the unknown. *Journal of Cellular Physiology*, 182, 311–322.
- Shu, T., Butz, K. G., Plachez, C., Gronostajski, R. M., & Richards, L. J. (2003). Abnormal development of forebrain midline glia and commissural projections in Nfia knock-out mice. *Journal of Neuroscience*, 23, 203–212.
- Song, H. R., Gonzalez-Gomez, I., Suh, G. S., Commins, D. L., Sposto, R., Gilles, F. H., ... Erdreich-Epstein, A. (2010). Nuclear factor IA is expressed in astrocytomas and is associated with improved survival. *Neuro-Oncology*, 12, 122–132.
- Steele-Perkins, G., Plachez, C., Butz, K. G., Yang, G., Bachurski, C. J., Kinsman, S. L., ... Gronostajski, R. M. (2005). The transcription factor gene Nfib is essential for both lung maturation and brain development. *Molecular and Cellular Biology*, 25, 685–698.
- Stringer, B. W., Bunt, J., Day, B. W., Barry, G., Jamieson, P. R., Ensbe, K. S., ... Richards, L. J. (2016). Nuclear factor one B (NFIB) encodes a subtype-specific tumour suppressor in glioblastoma. *Oncotarget*, 7, 29306–29320.
- Suwarnalata, G., Tan, A. H., Isa, H., Gudimella, R., Anwar, A., Loke, M. F., ... Vadivelu, J. (2016). Augmentation of autoantibodies by helicobacter pylori in Parkinson's disease patients may be linked to greater severity. *PLoS One*, 11, e0153725.
- Tamamaki, N., Yanagawa, Y., Tomioka, R., Miyazaki, J., Obata, K., & Kaneko, T. (2003). Green fluorescent protein expression and colocalization with calretinin, parvalbumin, and somatostatin in the GAD67-GFP knock-in mouse. *Journal of Comparative Neurology*, 467, 60–79.
- Tanga, F. Y., Raghavendra, V., Nutille-McMenemy, N., Marks, A., & Deleo, J. A. (2006). Role of astrocytic S100beta in behavioral hypersensitivity in rodent models of neuropathic pain. *Neuroscience*, 140, 1003–1010.
- Tsang, K. M., Croen, L. A., Torres, A. R., Kharrazi, M., Delorenze, G. N., Windham, G. C., ... Weiss, L. A. (2013). A genome-wide survey of transgenerational genetic effects in autism. *PLoS One*, 8, e76978.
- Vyazunova, I., Maklakova, V. I., Berman, S., De, I., Steffen, M. D., Hong, W., ... Collier, L. S. (2014). Sleeping Beauty mouse models identify candidate genes involved in gliomagenesis. *PLoS One*, 9, e113489.
- Wolf, H. K., Buslei, R., Schmidt-Kastner, R., Schmidt-Kastner, P. K., Pietsch, T., Wiestler, O. D., & Blumcke, I. (1996). NeuN: A useful neuronal marker for diagnostic histopathology. *Journal of Histochemistry & Cytochemistry*, 44, 1167–1171.
- Wong, Y. W., Schulze, C., Streichert, T., Gronostajski, R. M., Schachner, M., & Tilling, T. (2007). Gene expression analysis of nuclear factor I-A deficient mice indicates delayed brain maturation. *Genome Biology*, 8, R72.
- Zhang, Y., Chen, K., Sloan, S. A., Bennett, M. L., Scholze, A. R., O'Keefe, S., ... Wu, J. Q. (2014). An RNA-sequencing transcriptome and splicing database of glia, neurons, and vascular cells of the cerebral cortex. *Journal of Neuroscience*, 34, 11929–11947.
- Zheng, S., Eacker, S. M., Hong, S. J., Gronostajski, R. M., Dawson, T. M., & Dawson, V. L. (2010). NMDA-induced neuronal survival is mediated through nuclear factor I-A in mice. *Journal of Clinical Investigation*, 120, 2446–2456.
- Zhou, B., Osinski, J. M., Mateo, J. L., Martynoga, B., Sim, F. J., Campbell, C. E., ... Gronostajski, R. M. (2015). Loss of NFIX transcription factor biases postnatal neural stem/progenitor cells toward oligodendrogenesis. *Stem Cells and Development*, 24, 2114–2126.

**How to cite this article:** Chen K-S, Harris L, Lim JWC, et al. Differential neuronal and glial expression of nuclear factor I proteins in the cerebral cortex of adult mice. *J Comp Neurol*. 2017;525:2465–2483. <https://doi.org/10.1002/cne.24206>